APPLICATION OF PUROMYCIN-ASSOCIATED NASCENT CHAIN PROTEOMICS (PUNCH-P) TO PLANT SAMPLES

A Thesis Presented for the

Master of Science

Degree

The University of Tennessee, Knoxville

Aleksandra Izabela Noras

May 2020

ACKNOWLEDGEMENTS

I would like to thank my advisor, Dr. Albrecht G. von Arnim for his guidance throughout this project. I thank him for his instruction in logical experimental design, patience with my learning curves in plant biology, and ability to see at least one good thing about an otherwise unsuccessful experiment.

I also thank my lab members, Dr. Ansul Lokdarshi, Mark Edens, Ricardo Urquidi-Camacho, and Anwesha Dasgupta. Thank you all for being a joy to work with. Special thanks to Ansul and Ricardo for their assistance with my project, as well as past lab member Dr. Sung-Ki Cho for his preliminary work in PUNCH-P. I also thank Dr. Paul Abraham for his collaboration in performing all mass spectrometry experiments.

I thank my parents, Maciej and Kinga Noras for their support throughout my graduate school experience and occasional help with data analysis. I thank my fiancé Robert Tikkanen and his dogs, Maelstrom and Finn for their continuous cheer and loving support. I also thank my close friends Josh Sales and Rebecca Shrem and their cats Bourbon and Rosalind for letting me spend so much time at their apartment, especially during thesis writing.

ABSTRACT

Translation is a biological function present in all forms of life that allows for the production of proteins from strands of messenger RNA (mRNA). In plants, such as *Arabidopsis thaliana* or *Pisum sativum* (garden pea), translation is tightly regulated because of the plants' sessile nature and need to adapt to a variety of stresses. PUNCH-P is a proteomic technique that offers a snapshot of the translational status of cells in both a noninvasive and time sensitive manner. It was previously developed for mammalian tissues but had not been adapted to plants. PUNCH-P delivers an estimate of the rate of protein production using a technique complementary to ribosome foot printing or polysome loading. This method circumvents the in-vivo labeling needed for isotope-based mass spectrometric methods and avoids high sequencing costs associated with ribosome foot-printing methods.

Nascent peptides attached to ribosomes are isolated from a frozen tissue sample by centrifugation through a sucrose cushion. These peptides are then C-terminally labelled with biotin-puromycin. The incorporation of biotin allows for downstream peptide visualization on a western blot using streptavidin-horseradish peroxidase as a detection agent. Peptides may also be captured with streptavidin coated beads and analyzed via mass spectrometry (LC-MS/MS).

Here, I validate the PUNCH-P method for Arabidopsis and peas. It is well known that heat shock causes an overall decrease in the translational activity of plants due to mechanisms such as the sequestering of cytoplasmic mRNAs into stress granules and the shift to translating heat shock proteins (HSPs). This work presents methods to efficiently label, capture and detect biotin-labeled nascent peptides from plants. With heat treatment as a proof of concept, we show that puromycylation recapitulates the shift in the patterns of translation expected from polysome profiling. In addition, I show

preliminary data on the identity of the nascent proteins as identified by mass spectrometry. These advances suggest that PUNCH-P is a promising technique that can complement other proteomic and RNA-based methods to measure protein synthesis rates in plants.

CONTENTS

LIST OF TABLES

LIST OF FIGURES

1. INTRODUCTION TO PUNCH-P AND TRANSLATION

1.1 Translation Background

Transcription of organisms' DNA to RNA and the subsequent translation of RNA to protein is a crucial part of life and termed the central dogma of biology. Proper organismal function depends upon a series of tightly regulated mechanisms to guide the appropriate expression of genes not only throughout development, but also in response to stresses. Translational regulation acts as one such control mechanism. This is achieved by the fine-tuning of protein levels during cell proliferation and differentiation, as well as spatial and temporal regulation of protein expression [4]. Therefore, the study of translation is important in developing an understanding of the process of gene expression and how tightly it is controlled downstream of transcription.

Plants require the ability for fine-tuned translational control because of their sessile nature [5]. They depend on the ability to quickly respond to their environment and adaptation to adverse growth conditions [6]. The response plants have to stresses is also crucial to aquired tolerances which allow the plant to balance between growth and defense. Both growth and defense are energetically costly processes so it is crucial that plants optimize a balance between the two through processes such as translational control [7]. Much is yet unknown about the translational control of plants under stress. Translation remains a crucial process for study because of its many levels of regulation [8].

There are several ways in which the rate of translation, or translational efficiency may be modified. Here, translational efficiency refers to the number of protein molecules produced per mRNA molecule per unit of time [5]. The three phases of translation are translation initiation, elongation, and termination. Of these, translation initiation is

deemed to be the most commonly regulated process because it is the committed step and therefore rate limiting [9].

Translational initiation can be regulated at various points of this complex process, which involves the mRNA, ribosomal subunits and various translation initiation factors. The mRNA's 7-methyl guanosine (m7GpppN) cap is first recognized by the cap binding protein eIF4E, which is associated with a scaffold protein, eIF4G. The RNA helicase eIF4A and an RNA binding partner protein, eIF4B, assist with unfolding of the mRNA's 5' end. At this stage, the mRNA is considered to form a 'closed loop' due to interactions between the poly(A) binding proteins on the 3' end and eIF4G and eIF4B. Meanwhile, the 43S pre-initiation complex consists of the small ribosomal subunit (40S), a ternary complex (eIF2/GTP/Methionyl-initiator-tRNA), and the eukaryotic translation initiation factors eIF1 and eIF1A, eIF3, and eIF5. The mRNA, which is marked by the cap binding complex (eIF4E and eIF4G), is then be recognized and bound by the 43S pre-initiation complex. This then allows the 43S pre-initiation complex to scan the mRNA in the 5'–3' direction until the methionyl-tRNA recognizes a start codon (AUG). Next, the GTP of eIF2 is hydrolyzed, and most if not all of the initiation factors dissociate, the 60S ribosomal subunit is attached and translational elongation begins [8].

Translation elongation is mediated by a set of proteins termed elongation factors (eEFs) eEF1 and eEF2. eEF1 comprises eEF1A and eEF1B. eEF1A delivers aminoacyl-tRNA (aa-tRNA) to the ribosome in a GTP-dependent manner. Therefore, translational elongation is a highly energy dependent process and can be modified by the energy status of the plant. aa-tRNA availability also plays a role in the speed at which translational elongation may occur [10].

Commonly, the rate of translation of an mRNA is estimated from its polysome loading status, that is the number of ribosomes per mRNA, which can be measured by

biochemical fraction techniques. However, it is important to appreciate that the number of ribosomes alone is an imperfect measure of translation rate. After all, if elongation slows down, mRNAs will remain polysome-associated even when translational initiation is impaired. In addition, everything else being equal, long mRNAs will have more ribosomes than short mRNAs, although the rate at which ribosomes complete protein synthesis is the same. Therefore, the traditional method of measuring polysomes as a proxy for translational activity may be inaccurate.

The 7-methyl guanosine (m7GpppN) cap at the 5’ end of the mRNA and the poly(A) tail at the 3’ end promote translation by increasing the stability of the mRNA and by attracting the initiation factors [11] [12]. Translational efficiency may also be affected by the structure of the mRNA itself. The 5’ untranslated region (5’ UTR), has the greatest effect on ribosome loading based on nucleotide composition, length, predicted secondary structure, and the presence of untranslated AUGs [13]. Secondary mRNA structures such as hairpin loops may stall ribosomal scanning. The 3’ UTR or other regions of the mRNA may also interact with specific RNA-binding proteins, such as Pumilio-domain (Puf) proteins, or with miRNAs, which may affect RNA stability or translation. Thus, sequence features and structural features of the mRNA may affect its rate of translation.

Translational efficiency is also affected by the folding and degradation of proteins as they are being translated. This process is termed co-translational protein degradation or CTPD. Initially discovered using heavy isotope labeling techniques, this process relies on the N terminus of a translated peptide to be available to the proteasome for degradation before the translation of the protein is completed. This also refers to proteins that have left the ribosomal complex but have not yet been folded into their final tertiary or quaternary structure [14]. Ha et al.[14] show that this process preferentially

targets rapidly translated proteins in yeast. Their conclusions show that proteins that are more quickly translated show more CTPD effects due to the fact that rapid translation allows for more errors in the peptide chain. These peptide chains are then targeted for degradation before their translation is completed. This effect is also seen for polypeptides that are longer and that have unstructured N terminal regions. They conclude that this process is also unrelated to protein turnover events[14]. This phenomenon may be an area for consideration for PUNCH-P, as nascent peptides that have a biotin-puromycin incorporation into their C terminal end may yet be degraded from their N terminal end and affect peptide mapping and analyses.

1.2 Heat Stressed Plant Sample Rationale

Heat stress affects homeostasis within cells, leading to a delay in cell growth, cell damage or death of the organism [15]. Plants have a variety of methods of dealing with these exogenous stresses. As with other stresses such as hypoxia and heavy metals, changes in transcription, RNA maturation, translation, and transcript decapping and degradation are all available to alter the plant response to heat. At the level of translation [9, 15] changes in initiation and elongation (ribosome stalling) play a role translational regulation during heat stress [16].

A common response of plants to heat stress is a general collapse of polysome loading, which is caused by a block in initiation and is accompanied by sequestration of mRNAs into heat stress granules. While there is a global downregulation of translation in response to heat stress, not all protein translation is repressed in plants. It was found that mRNAs coding for relevant proteins involved in the general stress response are upregulated during heat stress, while mRNAs coding for proteins related with translation and ribosome biogenesis are globally inhibited. As laid out by Yangüez and coworkers [17], heat stress induced transcriptional regulators such as STZ/ZAT10 and DREB2B

remain translated and in turn affect downstream genes in Arabidopsis, some of which are known to enhance salinity, drought and heat stress tolerance in plants [17]. Yángüez et. al, also analyzed features of differentially translated genes under heat stress and found that the 5'UTR G+C content of mRNAs may predict increased or decreased (high GC) translation under stress [17].

The induction of heat shock proteins is part of plants' heat acclimation response and is necessary for the development of thermotolerance to ensure that basic cell functions are maintained [18]. Several classes of HSPs have been described in plants. They are named by their approximate molecular weights in kDa as HSP110, HSP90, HSP70, HSP60, and low molecular weight HSPs (15-30 kDa). HSPs are also found at significant levels in normal, non-stressed cells [18]. During heat stress however, heat shock proteins function as molecular chaperones that prevent protein misfolding and aggregation [17]. HSP70 and HSP40 specifically also play a large role in translation elongation, because they function as molecular chaperones to prevent the aggregation of nascent peptides as they exit the ribosomal exit tunnel [19]. They have also been found to help the plant to recover after stress and function in the disassembly of stress granules back into actively translating polysomes [19].

During heat stress as well as other stresses, plants modify what mRNAs are translated by sequestering them into cytosolic ribonucleoprotein structures called stress granules. While stress granules may contain some translation initiation factors, no active translation occurs [20]. Stress granules may also exchange mRNAs with processing bodies, whose mRNA contents are targeted for decapping and degradation [16]. Much is still unknown about the functional role of these sequestered mRNAs as well as how they are released from the P

body or stress granule [15]. However, HSP101 has been shown to assist in the re-solubilization of translation factors like eEF1B and eIF4A from stress granules during plant heat shock recovery [21].

In this work, I treated *Arabidopsis thaliana* and *Pisum sativum* seedlings with heat stress as a model system to examine the complexities of translational efficiency from a protein production perspective. I propose an emerging method, Puromycin-associated Nascent Chain Proteomics (PUNCH-P), to offer a snapshot of the translational status of a plant at a given time during treatment. PUNCH-P aims to answer the question of what kinds of proteins are being translated at a certain timepoint as well as how efficiently this is occurring, by measuring the identity and abundance of nascent chain polypeptides in cellular ribosomes. This method is not the only available way to study the translational efficiency of a plant sample. However, it serves as a new technique that may add to the robustness of results provided by various, mutually complementary, techniques. Techniques for studying translational status and efficiency will be compared and discussed in subchapter 1.4.

1.3 Principle of PUNCH-P

PUNCH-P is a methodology that allows for the monitoring of translation rates based on the incorporation of biotin-puromycin molecules into a growing peptide chain. This incorporation into the peptide chain is catalyzed in a non-sequence specific manner by the ribosome. The biotin-puromycin structure mimics the 3' CCA tail of a tRNA molecule and therefore can enter the ribosomal A site. It then undergoes a peptidyl transferase step where it is incorporated into the peptide chain found in the P site of the ribosome. Puromycin is incorporated into the C terminal end of a peptide chain via a peptide bond similar to the one formed upon transfer of a peptide from peptidyl t-RNA to the next aa-tRNA [2]. Due to the amide linkage found in this molecule, no amino acids or other biotin-puromycin molecules can be incorporated into the peptide chain after one biotin-puromycin has already been added [2]. At this point translation ceases. The structures of a tyrosine amino acyl tRNA and biotin puromycin are compared in Figure 1, panel A. A schematic of biotin-puromycin incorporation into a nascent peptide chain is shown in Figure 1 panel B.

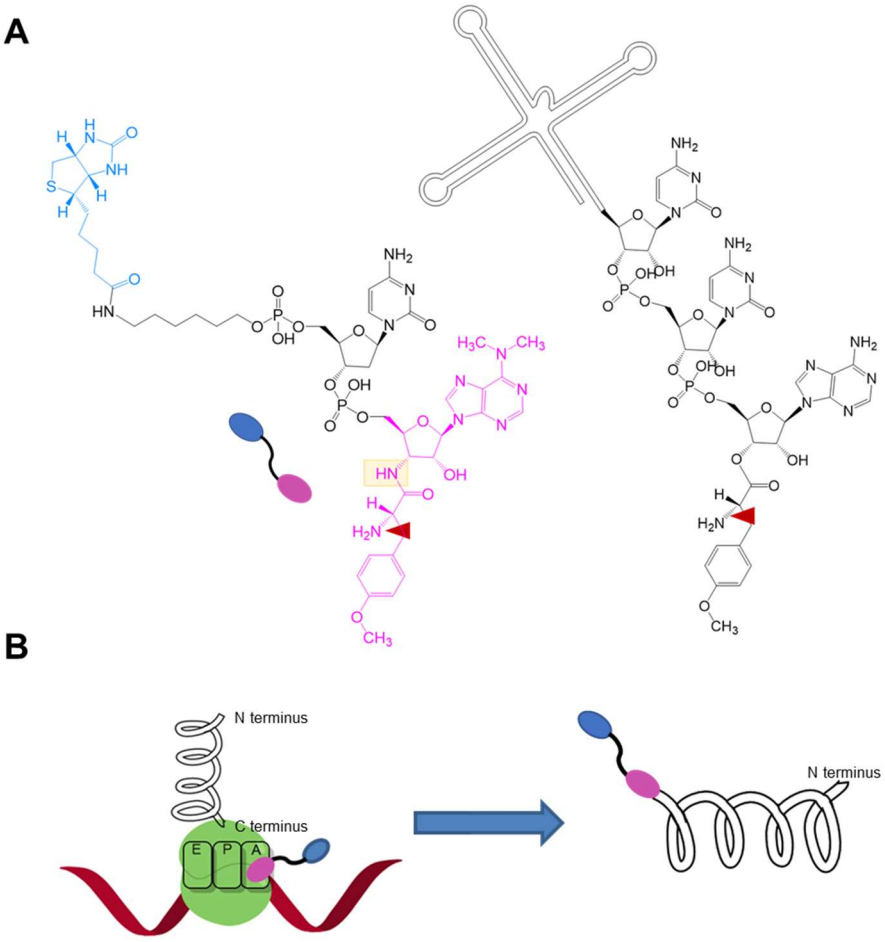

Figure 1: Schematic of Biotin-Puromycin Structure and Its Incorporation into a Nascent Peptide Chain.

A) Shows the chemical structures of biotin-puromycin and a tyrosyl-tRNA. Puromycin acts as a tyrosine mimetic based on its structural similarities to the C terminal end of a tyrosyl-tRNA. Adapted from Pestka et. al [2]. Amide linkage found in biotin-dc-puromycin is highlighted in yellow. Peptide bonds are shown with red arrows. The color abbreviations used here and in later schematics indicate puromycin as pink and biotin as blue with a black linker region.
B) Shows the mechanism of biotin-puromycin incorporation into a nascent peptide chain. Puromycin enters the A site of the ribosome and is incorporated into the growing peptide chain in a non-sequence dependent manner. When the peptide leaves the ribosome, it is labeled with the puromycin peptide bonded to its preceding amino acid, and the biotin moiety free for downstream applications involving streptavidin. Biotin puromycin is abbreviated based on the color scheme established in panel A.

The method of PUNCH-P involves the isolation of ribosomes after cell lysis. The lysate is centrifuged in order to remove cell debris. This is followed by ultracentrifugation overnight through a 45% sucrose cushion to concentrate ribosomes and polysomes. Free amino acids and translation factors are removed during the ultracentrifugation step, thus stalling translation [1]. Ribosomes isolated from the pellet of the centrifugation tube are resuspended and quantified using a microvolume spectrophotometer. From here, nascent peptides are reacted with biotin-puromycin. Biotinylated peptides are then either captured on a solid support with the biotin-specific affinity reagent streptavidin or visualized via western blotting using streptavidin as a probe. Captured peptides are analyzed by liquid chromatography tandem mass spectrometry (LC-MS/MS) [22]. This general workflow is shown in Figure 2.

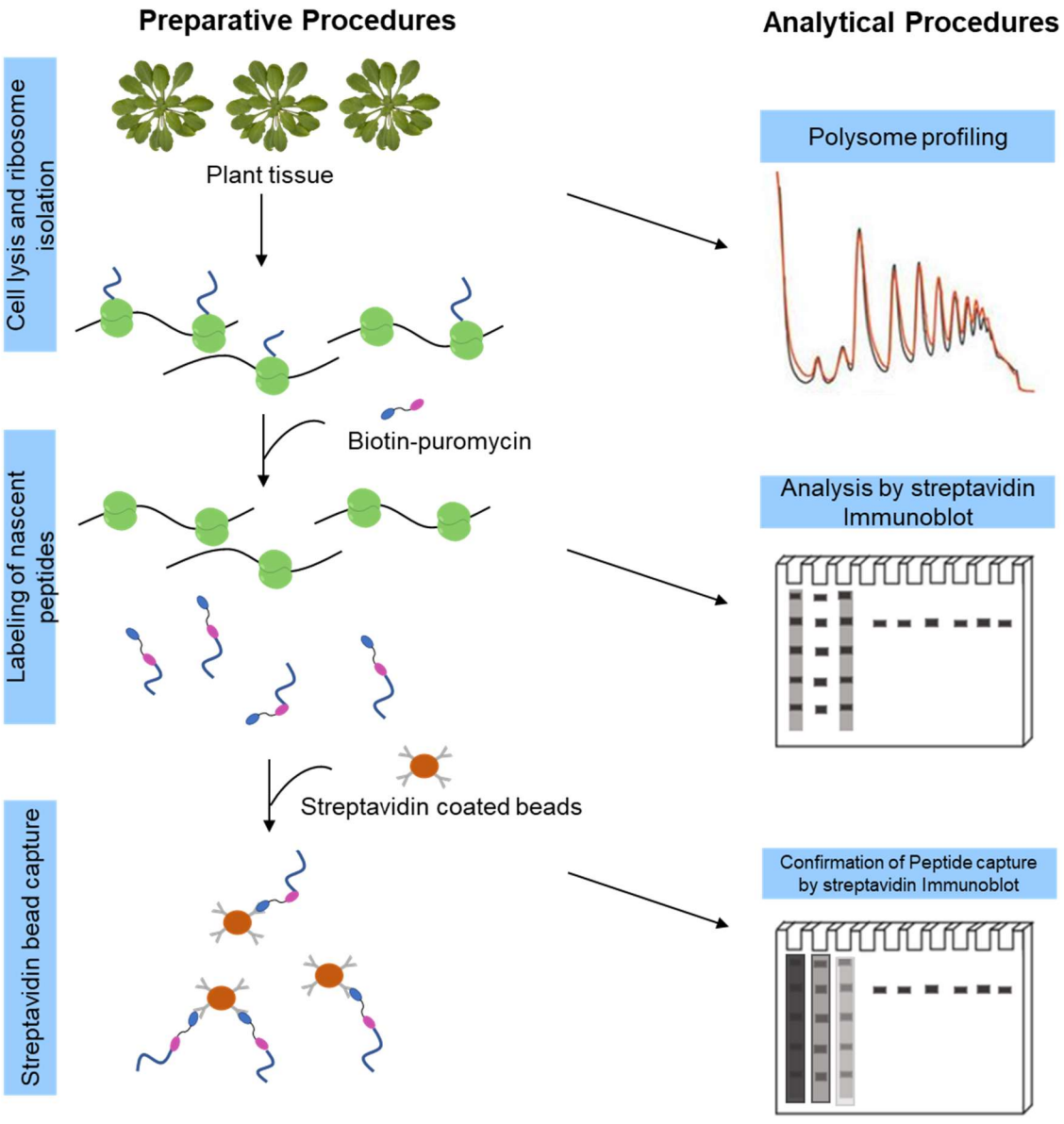

Figure 2: Outline of PUNCH-P Project Workflow.

Ribosomes and their attached nascent peptides are isolated from plant tissue. Their isolation from transcription factors and amino acids available in cells stalls translation. After extraction from tissue, ribosomes and nascent peptides may be analyzed by polysome profiling. These same ribosomal samples may also undergo a puromycylation reaction. Puromycylated peptides resulting from a puromycylation reaction were visualized with streptavidin probed immunoblots or captured on streptavidin coated bead for LC-MS/MS analysis. Adapted from Aviner et al [1].

1.4 PUNCH-P Rationale and Comparison to Traditional Methods of Translation

Many investigators, working in different species and cell types, have shown that cellular mRNA and cellular protein levels do not correlate perfectly, emphasizing the role of translational control and of protein turnover on overall protein expression levels [3, 22]. In fact, given simple assumptions, it can be deduced theoretically that mRNA levels should correlate with the protein production rate, rather than the total protein level. Because of the central role of gene expression in general, and protein synthesis specifically, for cellular function, it is reasonable to develop multiple methods for monitoring global translation rates. These methods quantify translation in two ways; either from a mRNA-driven or protein synthesis-driven perspective.

1.4.1 Polysome Profiling

Traditionally, polysome fractionation was used as a measure of the translational status of mRNAs present in a tissue [23]. The concept behind this is that the translation status of an mRNA is based upon its ribosome occupancy and ribosome density, both of which can be measured using this method. Loading of ribosomes onto mRNA is thought to represent the rate of protein production under the assumption that ribosomes are moving along the mRNA at the same rate [24]. While polysome profiling yields an estimate for rates of translation, this type of analysis does not perfectly correlate with overall protein production rates [25] because of the possibility of variable translation elongation rates.

1.4.2 SILAC

Stable Isotope Labeling by/with Amino acids in Cell culture (SILAC) involves the in vivo pulse labeling of nascent peptides with isotope labeled amino acids. Usually, ^{13}C leucine, or ^{15}N labeled amino acids are used, although radiolabeled amino acids such as ^{35}S methionine or cysteine can also be used. The isotope labeled amino acids are

monitored for their incorporation into newly synthesized proteins in comparison to unlabeled amino acids over a set period of labeling time. These resulting proteins are then detected by mass spectrometry (LC-MS/MS) or, if radiolabeled, by SDS-PAGE followed by autoradiography, densitometry, or scintillation counting [11]. In order to obtain an adequate signal using SILAC, the native amounts of amino acids must be depleted in the cells in order to be replaced by isotope labeled amino acids. This process is stressful for the cells and the time required for the exposure of cells to the isotope labeled amino acids limits the temporal resolution of the technique [1]. Another consideration is that labeled amino acids may not be taken up uniformly across the tissue, or the amino acids may be metabolized. These factors can lead to artefacts and inaccurate results in SILAC experiments.

1.4.3 BONCAT

Bio-orthogonal Noncanonical Amino Acid Tagging, or BONCAT is another method of amino acid labeling of a growing peptide chain, similar to SILAC. Here, the methionine analog azidohomoalanine (AHA) is fed to cells in vivo and incorporated into newly synthesized proteins. This circumvents the need for isotope labeled amino acids, as in SILAC. However, BONCAT also requires the stressful depletion of endogenous methionine before the addition of AHA. Once proteins are labeled with AHA, the cells are lysed, and a biotin tag is added directly to the incorporated AHA through a 'click chemistry' reaction. This allows for the capture of the proteins using the strong affinity of streptavidin for biotin. However, to date this method was only capable of detecting proteins on the order of hundreds, as compared to the thousands of proteins that are detectable by SILAC or PUNCH-P [25, 26].

1.4.4 Ribosome Footprinting

Ribosome foot printing (Ribo-seq) is a technique based on the deep sequencing of mRNA fragments that are protected by a ribosome stalled in the process of translation elongation [27]. For this method, mRNA–ribosome complexes undergo a nuclease treatment to remove the mRNA sequences unprotected by the ribosome. This leaves 25–33 nucleotide long ribosome protected mRNA fragments known as ribosome footprints [28]. These footprints can then be sequenced using next-gen sequencing to show what fragments of mRNA were translated at a certain timepoint. This method can resolve the position of ribosomes at the sub-codon level. Like PUNCH-P, Ribo-Seq does not involve cellular stresses due to isotope labeling or amino acid depletion. However, this method still predicts translation based on a snapshot of ribosome loading of mRNAs. Other drawbacks of ribo-seq methods are the time and cost intensive nature of RNA library preparation and deep sequencing.

1.4.5 SUnSET

Another puromycin based technique to detect the translational status of mRNAs is SUnSET or SUrface SEnsing of Translation. VanHoewyk et al [29] use this technique with hydroponically grown Arabidopsis seedlings, so that puromycin could be added to their growth media. By including puromycin into the growth media, the roots take it up. This puromycin is incorporated into the nascent peptide chains of translating proteins. The translational status of the plant is then determined using an anti-puromycin immunoblot, with an increase in puromycin signal in those plants that were more translationally active. This method provides a general overview of the translation status but does not provide detailed information as to the types of peptides that are translationally upregulated. Other areas of concern with puromycylation techniques include titrating the amount of puromycin so that there is no cellular toxicity induced.

1.4.6 PUNCH-P Advantages and Limitations

PUNCH-P offers a snapshot of translation rates as determined by the amount and type of nascent peptides attached to ribosomes at a given time. As such, this method has features of both RNA-based and protein-based methods, because I first isolate mRNAs loaded with ribosomes, but then quantify the proteins being synthesized rather than the mRNA. There are benefits of PUNCH-P over other more traditional ways of studying translation. The main advantage is the ability to arrest translation of proteins at a specific time point without *in vivo* labeling. This prevents the risk of incomplete molecule penetration into the cell as well as potential detrimental effects or stresses. *In vivo* labeling also requires a time window of exposure to the labeled molecules, thereby reducing the time resolution of the technique [1]. However, PUNCH-P has not been adopted as widely as other techniques and has not been documented in plants. A comparison of methods commonly used in translation analysis is shown in Figure 3.

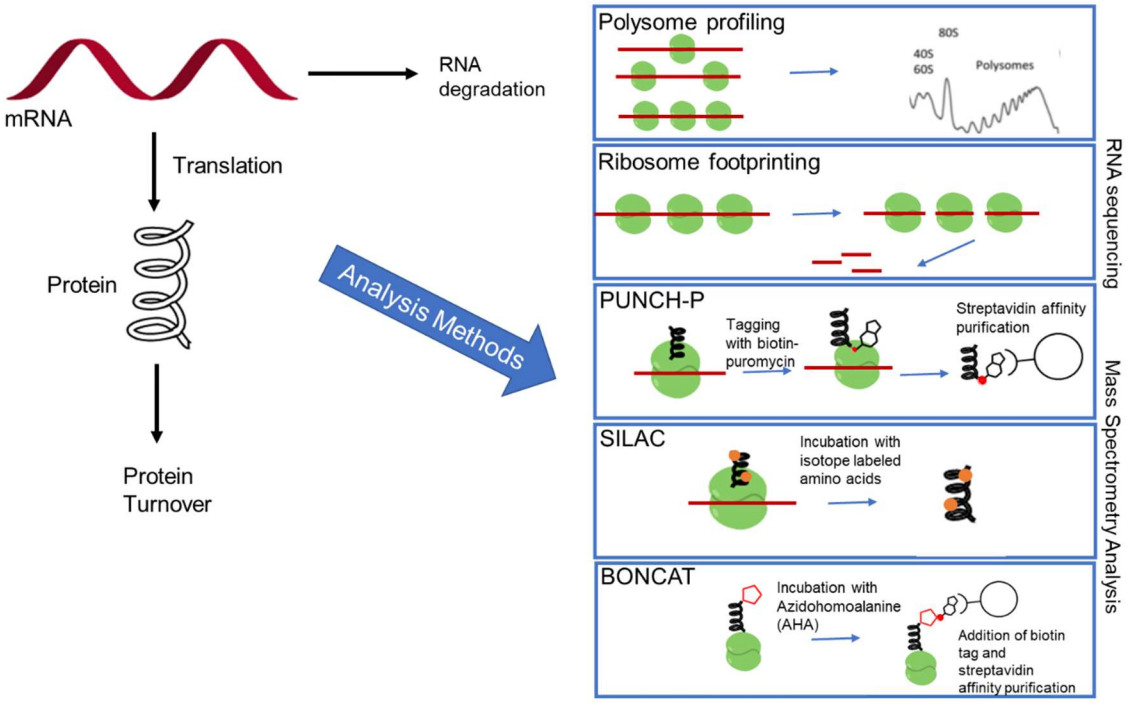

Figure 3: Comparison of Methods Used for the Study of Translation.

An illustration comparing the methods traditionally used for transcription analysis. These methods include approaches that focus both on protein production analyses as well as ribosome and mRNA focused techniques. All methods in this figure are discussed in subchapter 1.4. PUNCH-P and polysome profiling are the main techniques used for translational analyses in this work.

The main drawback for PUNCH-P is the large amount of plant sample required to generate enough nascent peptides for analysis using LC-MS/MS. According to Aviner et. Al. [3], ribosomes equivalent to at least 480µg of ribosomal RNA are required to detect and quantify a sufficiently large number of nascent proteins using LC-MS/MS. Puromycin may also truncate the production of proteins which may alter their stability for further analysis [3]. It is also unknown whether all peptides are equally labeled with puromycin, which may lead to biases in the proteins represented by LC-MS/MS results.

Figure 4 compares the three translational monitoring methods [1] based on data from HeLa cells. The reproducibility between two PUNCH-P experiments was high, as was also the case for two SILAC experiments. The authors note that the pairwise correlation of protein synthesis rates as determined by PUNCH-P with the SILAC and Ribo-Seq methods is low. Given that none of the techniques is justifiably superior over the others, PUNCH-P (as well as SILAC and Ribo-Seq) may thus provide new insights into translational regulation that complement the results of other techniques [3]. In fact, Aviner et al. [3] compared the effectiveness of PUNCH-P to riboseq in another work aimed at mammalian cells in their G1 and M phase. They conclude that both methods are complementary to one another and increase the translatomic data available compared to using one of these methods alone [3].

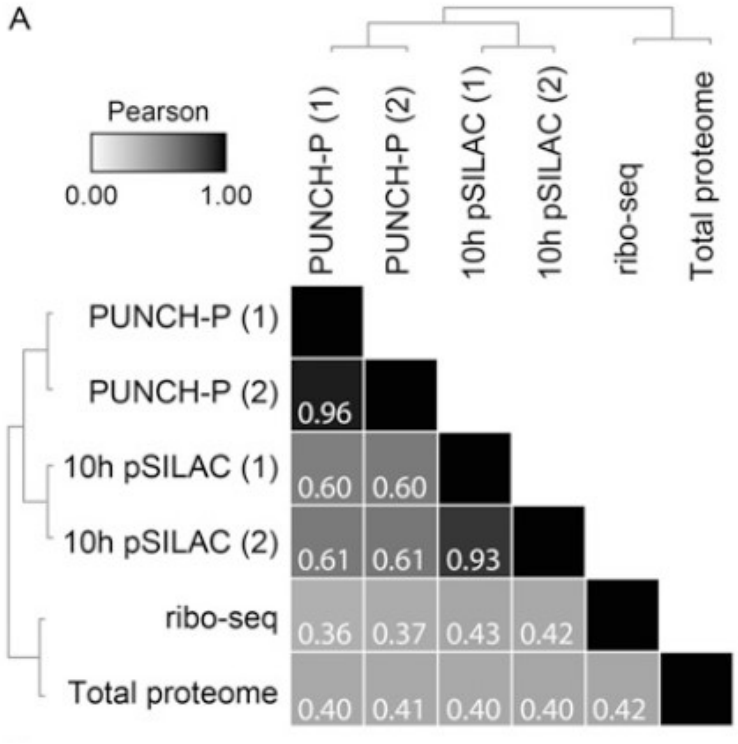

Figure 4: Comparison of Translation Monitoring Techniques.

A heat map comparing techniques of analyzing HeLa cell translatomes. PUNCH-P experiments were performed by Aviner et al and compared to other publicly available HeLa cell translatomes analyzed via pSILAC, ribo-seq and total proteome analyses [3]. The Pearson correlation values shown in the boxes above indicate the accuracy of detecting proteins or expressed mRNAs detected using PUNCH-P, pSILAC, ribo-seq and total proteome analysis.

1.5 Application of PUNCH-P to Heat Stressed Plant Samples

This methodology for PUNCH-P has been outlined for mammalian cells such as HeLa cells and mouse brain tissue but has not yet been published for any plant application. Aviner et al.[3] first developed and applied this technique to HeLa cells where using PUNCH-P, they were able to measure cell cycle-specific fluctuations in synthesis for 5000 proteins. They also identified proteins not previously implicated in cell cycle processes. When they applied this technique to mouse brain tissues, they were able to generate the first translational profile of a whole mouse brain [3]. In a following publication, Aviner et al describe the methods of this technique so that it can be applied to other biological samples [1].The goal of my project is to optimize and adapt PUNCH-P for use with plant samples, namely Arabidopsis and peas, in order to investigate the translational status of these tissues under stress. While mechanisms of translation and their inhibition due to heat stress are not the focus of this project, they provide a useful way to track the efficacy of PUNCH- P to visualize changes in translation.

1.6 Questions Addressed in This Work

This project focuses on the optimization of the PUNCH-P method for *Arabidopsis thaliana* and *Pisum sativum* through the following steps, focusing primarily on untreated rather than heat-treated samples. First, ribosomes harboring nascent peptides were extracted from ground plant tissue and quantified using a microvolume spectrophotometer. These ribosomes then underwent a puromycylation reaction where biotin-puromycin was incorporated at the C terminal end of the peptide. These samples were then analyzed using western blotting techniques to ascertain the efficiency of puromycylation. Polysome profiling was also used to confirm the translational status of the harvested plant tissue. Isolated biotinylated nascent peptides from ribosomal

samples were then captured on streptavidin coated beads for subsequent LC-MS/MS analysis.

2. METHODS

2.1 Plant Culture and Harvest

2.1.1 Arabidopsis Seedling Preparation and Harvest

Wild type *Arabidopsis thaliana* (Columbia ecotype) seeds were sterilized using a wash of 70% ethanol followed by a 10-minute incubation in sterilization solution (50% bleach, 0.01% Triton X 100). After sterilization, seeds were washed with sterile water to ensure that no bleach remained. Seeds were stratified for 48 hours in sterilized water at 4°C. After the stratification period, seeds were germinated on ½-strength Murashige-Skoog (MS) salt plant media (MP Biomedicals, cat # 2633024) with 0.65% Phytoagar (Bioworld, cat # 40100072-2) under a long-day cycle of 16 hr. light (80±10 μEin $m^{-2}s^{-1}$)/8 hr. dark at 27°C. On day 12, seedlings were placed into a 37°C plate incubator for varying lengths of heat stress treatments. All heat stress was done in the presence of light (13±7 μEin $m^{-2}s^{-1}$). Heat stress recovery was done by placing seedlings back into 27°C incubators. Seedling shoots and leaves were promptly harvested after their heat treatment using liquid nitrogen. This plant tissue was stored in -80°C until used in downstream experiments.

2.1.2 Arabidopsis Inflorescence Preparation and Harvest

Arabidopsis inflorescences were harvested from seedlings in all-purpose peat moss (PRO-MIX FLX Flexible Purpose Growing Medium) supplemented with 24-8-16 nitrogen-phosphorous-potassium fertilizer (Miracle-Gro cat# 2000992). Plants grew for approximately one month, or until inflorescences were fully blooming. Plants were grown in long-day cycle of 16 hr. light (80±10 μEin $m^{-2}s^{-1}$)/8 hr. dark at 22 °C and 50% humidity. Plants were heat stressed in an incubator at 37°C in light (42±5 μEin $m^{-2}s^{-1}$) and inflorescences were harvested by plucking them off the plant with sharp tweezers while

they were still within heat treatment conditions. The Arabidopsis inflorescences were stored at -80°C.

2.1.3 Pea Seedling Preparation and Harvest

Pisum sativum (green arrow cultivar) seeds were imbibed for 24 hours under constant running water. They were planted in vermiculite (Palmetto Vermiculite, size A2) and grown for 12 days under long-day cycle of 16 hr. light (80±10 μEin $m^{-2}s^{-1}$)/8 hr. dark at 22 °C. Heat treatment of peas was done in the same way as with Arabidopsis seedlings and inflorescences, in a 37°C incubator on the presence of light (42±5 μEin $m^{-2}s^{-1}$). Peas shoots were harvested by cutting shoots with scissors just above the soil line, taking care not to collect any imbibed seed tissue. Samples were frozen in liquid nitrogen and stored at -80°C.

2.2 Ribosome and Nascent Peptide Isolation

Plant tissue was ground into a fine powder with mortar and pestle for approximately 15 minutes while still frozen. A minimum of 1.5g of plant tissue was used for the experiments mentioned here. Plant tissue powder was suspended in a ribosome isolation buffer (200 mM Tris-HCl pH 8.4, 25 mM $MgCl_2$, 50 mM KCl, 1% deoxycholic acid, 2% polyoxyethylene 10 tridecyl ether, 40U/mL RNAsin Ribonuclease Inhibitor (Promega cat#N2515), 10x Halt Protease and Phosphatase Inhibitor Cocktail (Thermo Scientific cat#1861280), 1.4μg/mL pepstatin (Thermo Scientific cat#26305-03-3), 2μg/mL leupeptin (VWR cat#193476-89-7)). Per past optimizations, the amount of ribosome isolation buffer used should be twice the volume of sample powder (v/v). After a 30-minute incubation of plant tissue powder in the ribosome isolation buffer on ice, cell debris was removed via centrifugation (SA300 rotor, 2x15 min at 12,200 rpm). The resulting supernatant was layered over a 45% sucrose cushion (45% sucrose, 200mM Tris-HCl pH 8.4, 25 mM $MgCl_2$, 50 mM KCl, 0.1 mM DTT, 40U/mL Ribolock RNAse

inhibitor, 1.4µg/mL pepstatin, 2µg/mL leupeptin). 7.5 mL of plant extract was layered over 2.5 mL sucrose cushion in Beckman Coulter polyallomer tubes (Thin wall Polyallomer Tubes, BK331372). These tubes containing sample layered over the sucrose cushion were ultra-centrifuged in a SW41Ti swinging bucket rotor at 39,500 rpm at 4°C for 19 hours. The result of the ultracentrifugation was a pellet of ribosomes at the bottom of the tube. All liquid contents of the tube were removed using an aspirator, leaving only a sticky green pellet at the bottom of the tube. While on ice, the pellet was resuspended with ribosome resuspension buffer (50 mM Tris-HCl pH 7.5, 10 mM $MgCl_2$, 25 mM KCl, 40U/mL Ribolock RNAse inhibitor, 10x Halt Protease and Phosphatase Inhibitor Cocktail 1.4µg/mL pepstatin, 2µg/mL leupeptin) and let to incubate on ice for 30 minutes. After the incubation time, the resuspended pellet was transferred to an Eppendorf tube and was spun down using a tabletop centrifuge at 15500 rpm. The resulting supernatant containing ribosome and nascent peptides was isolated and stored at -80°C for further experiments. The remaining pellet was resuspended again and let to incubate on ice for multiple rounds of ribosomal elutions. All elutions were kept on ice and their RNA concentrations were determined using a microvolume spectrophotometer (Nanodrop). Total mass of ribosomes was calculated from the volume of the sample and the formula that 1ml of ribosomes at 1 A260nm absorbance unit (also called 1 Optical Density or OD unit) represents 40 micrograms of RNA.

2.3 Puromycylation Reaction

The puromycylation reactions were split into two categories: small scale and large scale. Small scale puromycylation reactions, such as those used for Western blotting, require approximately 20 ug or 0.5 OD of ribosomes. Reactions for mass spectrometry require at least 480 µg of ribosomes in order to produce interpretable levels of nascent peptides in downstream LC MS/MS analysis [25]. Samples were

thawed on ice, and once liquid, they were aliquoted into separate tubes. Biotin-dC-Puromycin (Jena Biosciences cat# NU-925-BIO-L) was added to the ribosomal sample for a final concentration of 0.001 mM. KCl was also added into the reaction mixture for a final concentration of 0.5M. As a control, non puromycylated (-P) reactions were also used, where KCl and sample were included in the reaction tube without any biotin-puromycin. The reactions were incubated at 37°C for 30 minutes.

2.4 Precipitation Reaction

The inclusion of KCl in small scale reactions increases sample volume and salt concentration, which is not ideal for SDS PAGE. Also, the puromycylation reaction uses excess biotin-puromycin which may interfere with downstream analyses. Therefore, proteins were precipitated with chloroform and methanol to eliminate salts and other impurities. This reaction concentrates the puromycylated peptide products into a pellet that can then be resuspended in SDS buffer prior to loading. After the puromycylation reaction, water and 3xSDS buffer with bromophenol blue were added to increase the volume of the reaction (typically 150μL total volume). The volume of the mixture at this point was determined to be one reaction volume (150μL). In order to isolate a protein pellet, 1/2 of a reaction volume of chloroform was added, and 2 reaction volumes of methanol. The mixture was briefly vortexed, and 1 reaction volume of water was added. The mixture was then centrifuged at 15000 rpm for 5 minutes. This resulted in a separation of the sample into an aqueous phase (top) and organic phase (bottom) with the protein pellet at the interface. Lipids separate into the organic phase and water-soluble molecules are separated into the aqueous phase of the reaction, with the peptide pellet at the interface of these two solvents. The top aqueous phase was removed without disturbing the protein pellet. One reaction volume of methanol was added, and the reaction was centrifuged again at 15000 rpm for 5 minutes. At this step, the protein

pellet was found at the bottom of the tube and slightly stained with bromophenol blue. All liquid is then removed, with extra care not to disturb the pellet. The protein pellet was then be resuspended in SDS buffer and loaded onto 12% acrylamide SDS PAGE gel. A Bio-Rad mini-PROTEAN setup was used for running all SDS PAGE gels (Bio-Rad cat# 1658000). Gels were made to be 1.5mm in thickness.

2.5 Western Blot

Puromycylation reactions containing reaction products from 40 µg of ribosomes (small scale reactions) were separated via a 12% SDS PAGE gel under denaturing conditions. Proteins were transferred onto an Amersham Protran 0.45µm nitrocellulose membrane (GE Healthcare cat# 10600003) at 100 V for 1 hour using a Bio-Rad-mini PROTEAN tetra wet transfer apparatus (Bio-Rad cat #170-3930) and transfer buffer (25mM Tris, 192 mM Glycine,20%(v/v) Methanol). The membrane was stained with Ponceau S solution (2% solution in 2% acetic acid) in order to visualize transfer efficiency. The membrane was washed of this stain with water for 5 minutes followed by 5 minutes of TBS-T (Tris buffered saline with 1% Tween-20) wash. The membrane was blocked with bovine serum albumin (BSA) 7.5% solution in TBS-T at 4°C overnight or for 1 hour at room temperature. After blocking, the membrane was washed for 5 minutes at room temperature with TBS-T to remove any remaining BSA. The membrane was then incubated with a 1:16000 dilution of streptavidin-horseradish peroxidase (HRP) (Cell Signaling Technology cat# 3999S) in TBS-T for 1 hour at room temperature. It was washed for 1 hour using TBS-T, changing buffer every 10 minutes. The blot was developed using Advansta Westernbright chemiluminescent substrate (Advansta cat# K-12042-D10). For developing one 4x6cm blot, 200uL of each substate component were mixed in a dish. Then this mixture was dripped over a clean surface and the blot was swiped over the substrate mixture, protein binding side down. The blot membrane was

then put into a transparent plastic pocket made from a clear page protector, and excess substrate was squeezed out of the pocket. Blots were immediately imaged using a Bio-Rad Chemidoc MP luminescence imager. These images were then analyzed using the Bio-Rad Imagelab software.

2.6 Quantification of Puromycylated Peptides on Immunoblots

Puromycylated peptides were quantified using Bio-Rad Imagelab software (version 6.0.1). Upon import of the image to the Imagelab software, the image was straightened and cropped using the Image Tools function. Individual lanes of the blot were selected using the "volume" tool, specifically the lane drawing option. Lane sizes were kept consistent by copy/pasting the volume tool shape. This was needed for accurate comparisons of lanes on the blot. During this time, lanes containing only loading buffer were also selected to serve as a background blank. The luminescence value of these lanes was subtracted from each sample lane during quantification. In the case of any Western blot artifacts such as spots or smears, their volume was removed from quantified lanes using a freehand drawing tool. The volume values, meaning the area under the curves generated by sample signal, were exported to MS Excel for further analysis.

Each blot in this work contains a standard curve of biotinylated Bovine Serum Albumin (BSA) (Thermofisher cat#29130). It is recommended to have a standard curve present on each blot for analysis because of variations in transfer efficiency and optimal exposure time between blots. The intensity of biotinylated BSA signal were plotted against their protein concentrations (range from 40 to 0.3 ng) to generate a standard curve. A second order polynomial curve was best for fitting data points of biotinylated BSA lanes. This curve was then used to quantify the remaining lanes on the blot.

One benefit of using the Image lab program in combination with the Chemidoc MP is that the program automatically highlights areas of saturated signal. These areas would not be used for quantification, or a shorter exposure time would be chosen. This feature resolves previous concerns of oversaturated signal obtained from using X-ray film for western blot imaging. .

2.7 Polysome Profiling

Plant material was finely ground using liquid nitrogen and mortar and pestle. It was found that polysome yields increased with increased sample grinding time, with 15 minutes of grinding being optimal for yielding fine plant tissue powder. 0.5g of plant material was weighed into tubes and was resuspended in resuspension buffer (200mM Tris-Cl pH 8.4, 50mM KCl,1% deoxycholic acid, 25mM $MgCl_2$ 2% Polyoxyethylene 10 tridecyl ether, 400U/mL RNAsin, 50 µg/mL cycloheximide). The homogenate was centrifuged for 5 min at 20,000 rpm for 5 minutes. This centrifugation was done twice to ensure a transparent green supernatant. Upon removal of cell debris, the green transparent supernatant was loaded onto a 50% to 15% continuous sucrose gradient (15% or 50% sucrose, 200 mM Tris-Cl pH 8.4, 50 mM KCl, 25mM $MgCl_2$, 0.1mM DTT, 50 µg/mL cycloheximide) and ultra-centrifuged for 4 hours at 39,000 rpm in a SW41Ti swinging bucket rotor. The resulting polysome gradient tubes were kept at 4°C. For polysome gradient analysis, the polyallomer tube was pierced from the bottom using an ISCO Density Gradient Fractionator (Instrumentation Specialties Co. Model 185). The system pumped a 70% sucrose solution with bromophenol blue at a rate of 0.75 ml/min through the piercing needle and into the polyallomer tube, displacing the polysome gradient through the top of the tube towards a UV spectrophotometer. Sample absorbance was recorded in arbitrary units (AU) at 254nm, generating the polysome profile.

2.8 Streptavidin Bead Capture of Biotinylated Peptides

For bead capture and downstream LC-MS/MS analysis, a large scale puromycylation reaction was prepared. Upon reaction completion, the reaction mixture was filtered through a Zeba 7k MWCO desalting column (Thermo Scientific cat#87766S) to eliminate excess biotin-puromycin that was not incorporated into a peptide chain. Then, ribosomes and peptides were denatured through addition of urea-SDS buffer (8M urea, 2%(w/v) SDS, 200mM NaCl, 50 mM Tris-HCl) for a final concentration of 2 M urea. The sample mixture was heated at 65°C for 5 minutes. The denatured peptide solution was incubated with M280 Dynabeads (Invitrogen cat# 1205D) which have been washed and prepared according to manufacturer instructions in TBS buffer. The beads and sample mixture were incubated for 30 minutes at room temperature on a tube rotator. After incubation, the supernatant with unbound proteins was loaded onto an SDS-PAGE gel and immunoblotted to determine the efficiency of capture. Here, an absence of signal shows that peptides are bound to beads. Wash steps may also be saved and loaded onto an SDS-PAGE gel to determine their efficiency and the efficiency of binding.

The beads were then washed in a series of stringent wash steps to remove any nonspecifically bound proteins. All wash steps were done at room temperature and follow the bead wash steps outlined by Aviner et. al. 2014 [1]. 1 mL of urea-SDS buffer was used to wash the beads for 30 min on a tube rotator. After this period, supernatant was discarded. Beads were washed using 1 mL of urea-SDS buffer and were resuspended using a pipette tip for a total of five washes. Beads were then tumbled in 1 M NaCl for 30 min. After this step, beads were resuspended in 1 mL of 1 ml of 1 mM DTT. double deionized water, for a total of five washes. Then beads were tumbled for 30 min in 1 ml of 50 mM iodoacetamide. After this, beads were washed once in 1 mL 50 mM ammonium bicarbonate, supernatant was removed, and beads were stored in

another 1 mL of 50 mM ammonium bicarbonate in a fresh Eppendorf tube at 4°C for trypsin digestion and LC-MS/MS analysis. Wash steps, especially the first, may also be saved and loaded onto an SDS-PAGE gel to determine their efficiency and the efficiency of binding.

2.9 Peptide Digestion and Proteomic Analysis

Streptavidin beads with attached peptides were adjusted to 10 mM dithiothreitol for 30 min at 37 °C and cysteines alkylated with 30mM iodoacetamide for 15 min in the dark at room temperature. Proteins were digested by adding a 1 microgram aliquot of sequencing grade trypsin (Promega) to each sample followed by incubation on a thermal mixing block overnight at 37 °C. Peptides were desalted on Pierce C18 spin columns (Thermo Scientific) as per the manufacturer instructions. All samples were analyzed on a Q Exactive Plus mass spectrometer (Thermo Scientific) coupled with an automated Vanquish UHPLC system (Thermo Scientific). Peptides were separated on an in-house-pulled nano spray emitter of 75µm inner diameter packed with 30cm of 1.7µm of Kinetex C18 resin (Phenomenex). For each sample, a single 2µL injection of peptides was separated by a linear gradient from 2 to 22% of mobile phase B (0.1% formic acid, 80% acetonitrile) at a flow rate of 250 nL/min over 180 min. Mass spectra were acquired with the Q Exactive Plus instrument in a top 10 data-dependent acquisition setup. Full scan mass spectra were collected within 300 to 1500 m/z with automatic gain control (AGC) target value of 3 × 106 at a resolution of 70,000 with a maximum injection time (IT) of 25 ms. Precursor ions with charge states ≥2 and ≤ 5 and intensity threshold of 1.6×10^5 were isolated using a 1.6 m/z isolation width for higher-energy C-trap collision dissociation (HCD) with a normalized collision energy of 27 eV. MS/MS spectra were acquired at a resolution of 17,500 at m/z 200 with an AGC target value of 1×10^5 and maximum IT of 50 ms. Dynamic exclusion was set to 20 s to avoid repeated sequencing

of peptides. All resulting MS/MS spectra collected were processed in Proteome Discoverer, version 2.4 with MS Amanda and Percolator. Spectral data were searched against the *Pisum sativum* v1 reference proteome database with common laboratory contaminants appended. The following parameters were set up in MS Amanda to derive fully tryptic peptides: MS1 tolerance = 5 ppm; MS2 tolerance = 0.02 Da; missed cleavages = 2; Carbamidomethyl (C, + 57.021 Da) as static modification; and oxidation (M, + 15.995 Da) as dynamic modifications. The percolator false discovery rate (FDR) threshold was set to 1% at the PSM and peptide levels. FDR-controlled peptides were then quantified according to the chromatographic area-under-the-curve and mapped to their respective proteins. Peptide abundances were summed to estimate protein-level abundances.

2.10 PUNCH-P LC-MS/MS Data Analysis

Peptides detected by LC-MS/MS were identified by their molecular weights. These peptides were then mapped to their respective protein match in the pea genome. Peptide presence and abundance was identified in each of the samples provided to collaborators. For ease of analysis, peptides were sorted from most to least abundant, and assigned a number to help with their identification. FASTA sequences of proteins matched by the peptides detected were found using the Legume Information Service(LIS) [30]. The BLAST-P Sequence analysis tool was used to align FASTA sequences found in the LIS to PUNCH-P detected peptides of puromycylated and non puromycylated samples [31]. These peptides were then mapped to the FASTA sequence of their protein match, based on a minimum 90% identity match. Proteins with transit peptides from those detected were identified referencing Chotewutmontri et al [32]. This article references proteins from Arabidopsis, however, *Pisum sativum* analogues that were found in PUNCH-P mass spec results were found also using LIS. In

order to find the transit peptide regions of proteins of interest, ChloroP, chloroplast transit peptide prediction server(version 1.1) was used [33]. All GO cell compartment terms for proteins matched were found manually using the UniProt database (release 01_2020) [34].

Proteins detected via mass spec were sorted into groups based on their presence in puromycylated versus non puromycylated samples. The same was done for the peptides detected in each sample. Files containing peptide and protein abundances in PUNCH-P samples may be found in the attachments titled Noras Thesis Supplemental 2020 which are related to this work.

3. RESULTS

The goal of this project was to adapt and optimize PUromycin-associated Nascent Chain Proteomics (PUNCH-P) for plant samples as an alternative method to characterize mRNA translation states. Preliminary work conducted prior to my joining the project had established that isolated plant ribosomes were indeed competent to incorporate a biotin-derivatized puromycin into nascent peptides *in vitro*. However, the yield of ribosomes, and thus the yield of puromycylated peptides, obtained from Arabidopsis seedlings and Arabidopsis inflorescences was low.

3.1 Pea Seedlings Yield More Ribosomes than Arabidopsis

In an attempt to explore other plant tissue types, it was found that pea seedlings yield almost 10-fold more ribosomes per gram of plant tissue than Arabidopsis seedlings and also yield more ribosomes than Arabidopsis inflorescences (Fig. 5), using the same ribosomal isolation method. These results were the motivation to later use pea ribosomes for bead capture experiments and optimizations, since large amounts of ribosomal material are required to generate enough nascent peptides to identify individual proteins by LC-MS/MS.

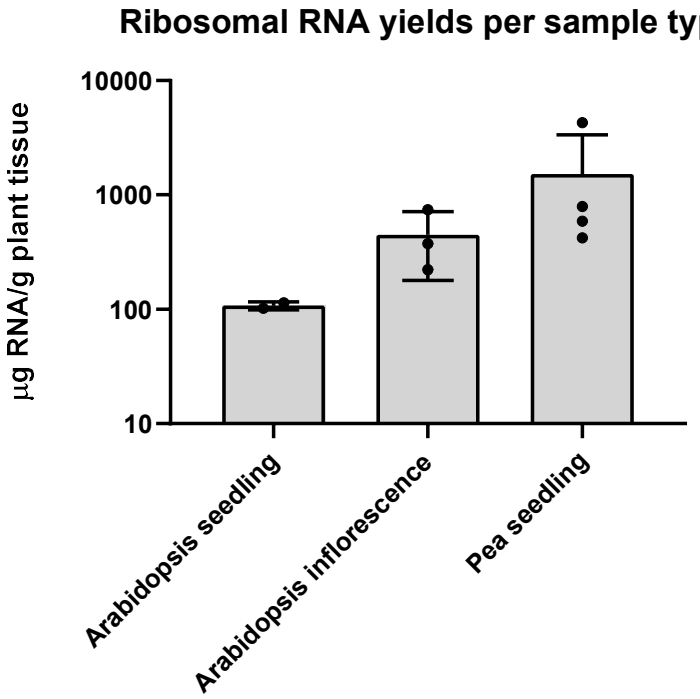

Figure 5: Comparisons of Ribosomal Yields Between *Arabidopsis thaliana* and *Pisum sativum* Plant Tissues.

Plant tissues were analyzed for the amount of ribosomal RNA yield per gram of fresh weight plant tissue. All plant tissues underwent the same ribosomal isolation protocol described in section 2.2. Seedlings analyzed were 12 days old.

Data points show individual biological replicates. Error bars represent standard deviation.

Y axis is represented with a log scale.

3.2 Polysome Profiles in Response to Heat Treatment

The degree to which ribosomes are engaged in translation of mRNAs can be determined by sucrose density gradient centrifugation of total cell extracts (polysome profiles). Arabidopsis and pea seedlings were subjected to 120 min heat shock (HS at 37ºC) followed by a 30 min recovery at normal temperature (22ºC) in order to establish whether heat treatment results in a global decline in translational activity. As shown in Figure 6, polysome profile experiments with pea seedlings confirmed the decrease of polysomes after 120 min of heat shock and the return to normal polysome loading during recovery (Fig. 6B, C). This is indicated by a flattening of the peaks in the polysomal region of the gradient upon heat stress. This polysomal collapse was quantified by calculating a polysome to monosome ratio (P/M) (Fig. 6C). In contrast to pea seedlings, polysome collapse in Arabidopsis seedlings was less pronounced under these conditions (Fig. 6A, C). These data are consistent with previously published results (e.g. Merret et al. [35]).

One troubleshooting factor to note is that the amount of signal in the polysome gradient is increased by the amount of time seedling samples are ground. This is most likely because more cells are lysed and available for RNA extraction. Polysome profiles were standardized by the amount of sample ground and resuspended in extraction buffer as well as maintaining the same amount grinding time for each sample.

Maintaining a stable detector baseline was another factor affecting reproducibility, which was addressed by running deionized water through the flow cell of the UV absorbance detector before setting a baseline. Here, baseline height is also variable due to later manual alignment of individual polysome gradients during analysis. This alignment is based on the initial rise of absorbance in the polysome gradients as they first enter the flow cuvette of the spectrophotometer.

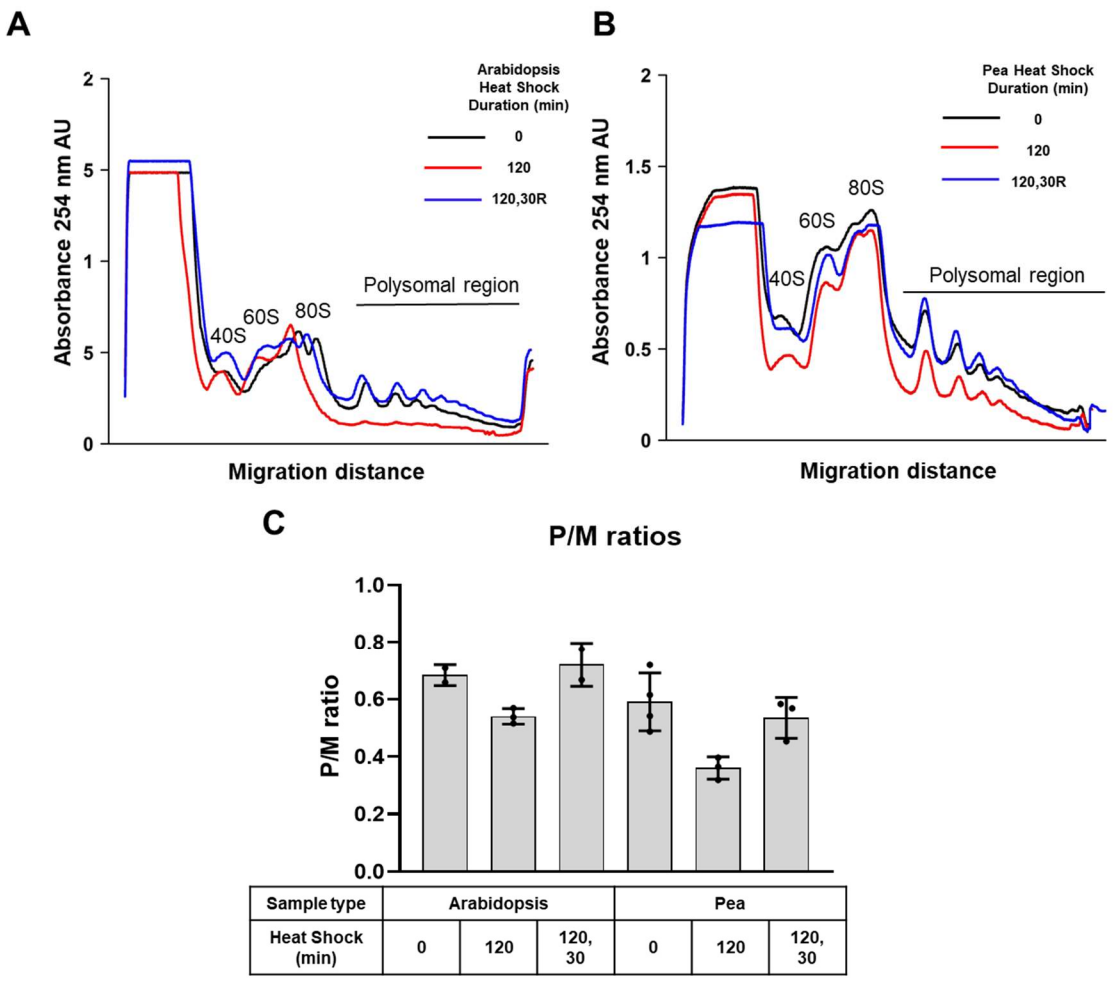

Figure 6: Polysome Profiles of Arabidopsis and Pea Samples.

A) Polysome profiles of *Arabidopsis thaliana* 12-day-old seedlings (sensitivity=0.5) n=3 replicates.
B) Polysome profiles of 12-day-old *Pisum sativum* seedlings (sensitivity=2) n=3 replicates.
Panels A and B show average polysomal profiles for each sample type. The y-axis indicates the continuous absorbance that was measured during the fractionation of the gradient, which reflects the concentration of RNA. The x-axis represents the migration distance traveled by the RNA through a 15% to 50% continuous sucrose gradient. The 40S, 60S and 80S monosome peaks are indicated. The polysomal region of the gradient is indicated with a line above the profile. Given that pea absorbance was recorded at a lower sensitivity setting, pea yielded about 10-fold more signal than Arabidopsis.
C) Comparison of polysome to monosome (P/M) ratios of Arabidopsis and pea seedlings. The monosome region encompasses the 40S, 60S and 80S regions. A decreased P/M ratio indicates a polysomal collapse with heat stress.

3.3 Puromycylation can be Detected by Streptavidin Blotting

Arabidopsis seedlings were grown at 22ºC, ribosomes were isolated through a sucrose cushion, and ribosomes were incubated with biotin-dC-puromycin (Bio-puromycin) as described in Methods in order to label nascent peptides. In order to visualize puromycylated peptides, peptides were separated using an SDS-PAGE gel. The gels were then immunoblotted (western blot) and probed using streptavidin conjugated with horseradish peroxidase (HRP) (Fig. 7). The puromycylated peptides appear as a smear of peptides of varying size because hundreds of polypeptides are puromycylated at different stages of translation. Bands shown in sample lane 3 where no biotin-puromycin was present in the reaction are a result of naturally occurring biotinylated proteins present in Arabidopsis seedlings. Endogenously biotinylated proteins in plants include mainly biotin dependent carboxylases. The molecular weights of these are described in Table 1 [36]. However, many of the bands shown in Fig. 7 are smaller than the ones reported in literature. This may indicate that there are other less studied biotinylated plant proteins present in plants. Many biotin-tagged proteins are also above the molecular weights accessible to immunoblotting experiments. Upon denaturation with SDS, it may be that only small biotinylated subunits of these larger proteins are visible. In summary, these results demonstrate that nascent proteins from Arabidopsis seedlings can be tagged and detected with biotin-puromycin.

Table 1: Endogenously Biotinylated Plant Proteins

Protein	Subunits	Molecular Weight (kDa)
Heteromeric Acetyl CoA Carboxylase (ACCase)	BC	50
	BCC	22-37
Homomeric Acetyl CoA Carboxylase (ACCase)	2 identical subunits	500
3-Methylcrotonyl-coenzyme A carboxylase (MCCase)	MCC-A	75-80
	MCC-B	60
Geranyl-CoA carboxylase (GCCase)	n/a	122
Seed Biotin Protein (SBP)	n/a	50-65

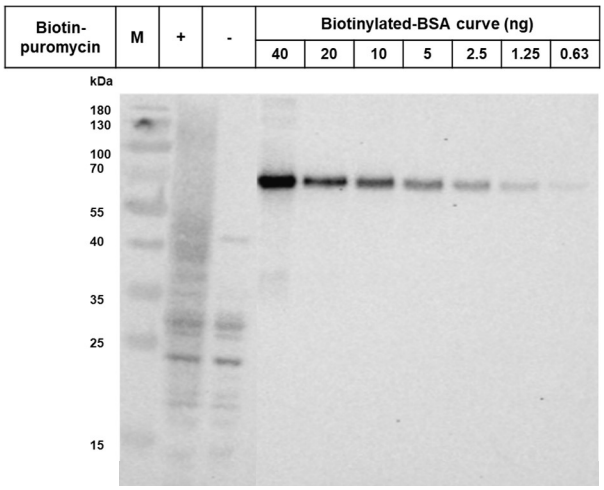

Figure 7: Representative Streptavidin Immunoblot of Puromycylated and Non-Puromycylated *Arabidopsis thaliana* Samples.

Arabidopsis ribosomes were incubated with biotin-tagged puromycin (+) or a negative control (-) and resolved by SDS PAGE and immunoblotted. Biotin was detected using streptavidin-HRP as a probe. The negative control reveals a series of specific bands that represent endogenously biotinylated proteins, as compared to the smear of peptide signal in puromycylation reaction. Biotinylated bovine serum albumin (BSA) was used as a standard curve for subsequent quantification of sample lanes.
M= molecular size marker.

3.4 Inclusion of KCl Enhances Puromycylation

In preliminary work for this project, KCl was included in puromycylation reactions, however, this was not mentioned in the original PUNCH-P protocol from Aviner et.al [1]. Figure 8 confirms that 0.5M KCl does increase the yield of puromycylation reactions by approximately 2-fold (Fig. 8A, C), which is not due to unequal loading of the gel (Fig. 8B). This addition of KCl to reactions containing puromycin has been studied previously, where high concentrations of KCl increase the function of puromycin. It is hypothesized that the increase in K^+ ions change the shape of the ribosome so that transitions of molecules between the A and P site of the ribosome are facilitated [37]. The result in Figure 8 suggests that KCl should be included in the puromycylation reaction in order to maximize peptide yield for peptide bead capture and LC-MS/MS analyses.

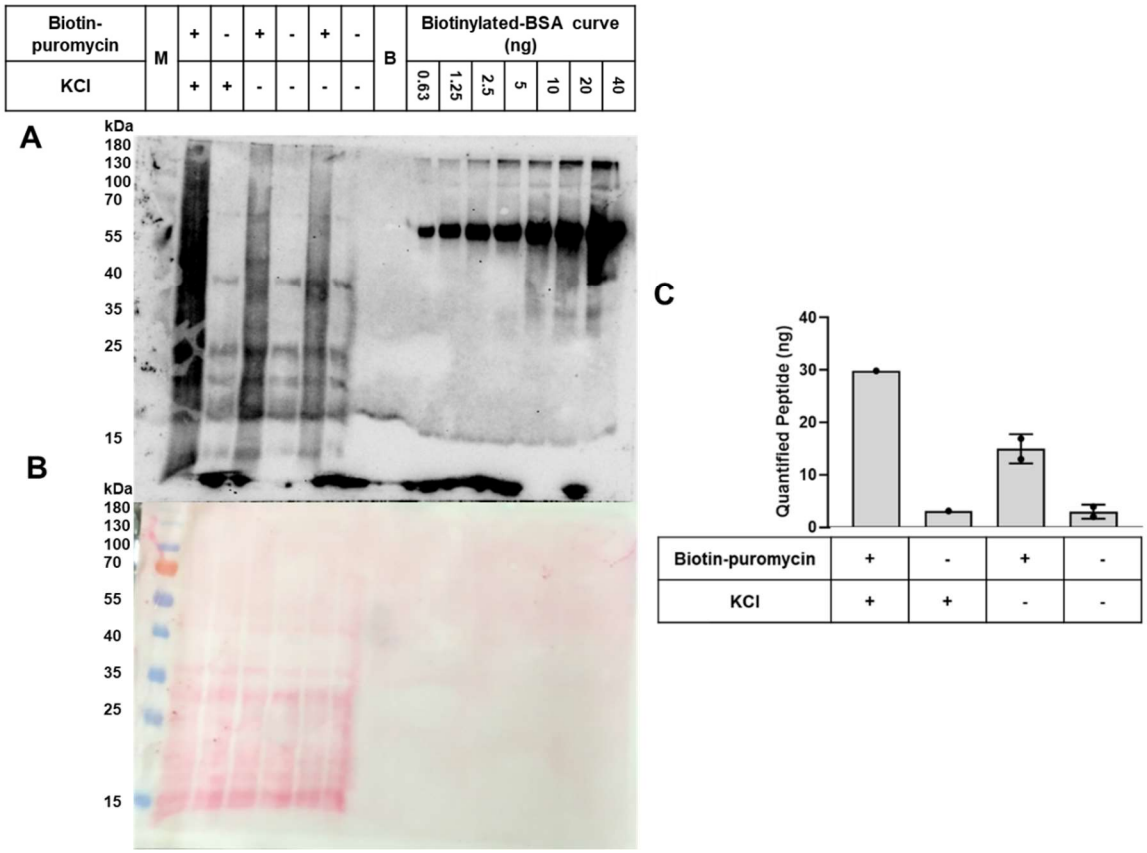

Figure 8: KCl Increases the Yield of Puromycylation Reactions.

A) Immunoblot of puromycylation reactions visualized with streptavidin-HRP immunoblotting. Lanes containing no biotin-puromycin served as a negative control.

B) Ponceau S stain of the blot in (A). The signal represents the proteins present in the ribosome preparation.

C) Quantifications of Arabidopsis sample lanes from A). n=2 for KCl absent experiments as indicated by lanes 4-7 from left in A.

M= molecular size marker.

3.5 Heat Shock and Subsequent Recovery Alter the Spectrum of Puromycylated Nascent Peptides

After western blot protocol was established and reproducible, the next investigation was to see whether amount of puromycylated peptides would be affected by the heat shock treatment. Figure 9 C and D details the qualities of heat treated samples that underwent puromycylation. As seedlings were exposed to a longer heat treatment their amount of puromycylated peptides decreased. A decrease in ribosome amount is also seen in Ponceau stains shown with heat treatment. In 120 minute heat treated samples, there is a band at approximately 70 kDa. This band is believed to be heat shock protein 70 (HSP70). 120 minute heat treatment with 30 minute recovery sample has a partially recovered puromycylated peptide amount as compared to untreated controls

In order to more easily compare the differences in banding patterns produced by puromycylated heat treated samples, lane profiles of the blot lanes were created. In Figure 9 A and B, the peaks show the intensity and locations of immunoblot bands in C and D. The left of the peak profiles corresponds to the higher molecular weight peaks at the top of the blot, and the right side to the low molecular weight peptides. Peak height corresponds to the band intensity on the blot. With heat treatment, the peak heights in the mid region of the blot diminish, indicating that the translation of these peptides is diminished, which also corresponds to the lighter smear of peptides in non puromycylated lanes. However, some peaks of the non-puromycylated lanes persist, again indicating the bands of the endogenously biotinylated plant peptides. A and B show two replicates of the same experiment, with peak profiles remaining similar between replicates.

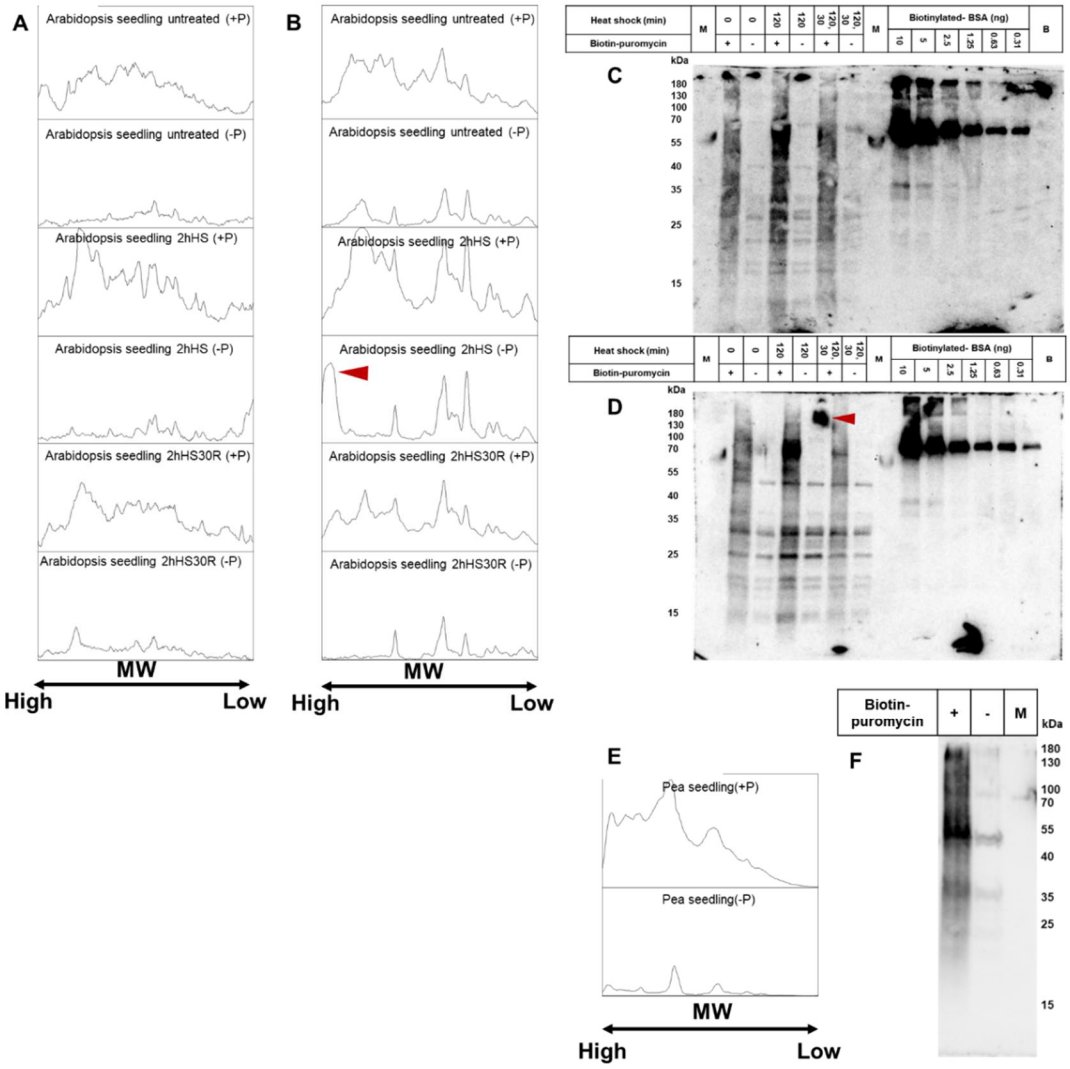

Figure 9: Puromycylation Profiles of Arabidopsis and Pea show Banding Patterns of Heat-Treated Samples.

A) and B) are puromycylation profiles based on the band locations and intensities in figures C) and D) respectively. These panels represent two biological replicates of heat-treated Arabidopsis 12-day seedlings.

E) Puromycylation profile of F) immunoblot bands of 12-day pea seedling samples.

M= molecular size marker.

B= blank lane

Red arrows in the figure denote an artifact of the blot that should be disregarded as it is not true sample signal.

3.6 Quality Control and Optimization Experiments

3.6.1 Free Biotin-puromycin Does Not Generate Spurious Signals

Because the puromycylation reactions contain an excess of biotin-puromycin, a concern was whether signal may be caused by unincorporated biotin-puromycin. To test this, ribosomes with their nascent peptides were denatured with SDS loading buffer before adding biotin-puromycin. With this denaturation, biotin-puromycin cannot incorporate into the nascent peptide chain. Figure 10 shows that no additional signal is generated by nonspecific interactions between biotin-puromycin and the proteins in the sample. Based on these results, the only signal produced on these blots is that from peptides with a biotin present, whether that be from a biotin-puromycin molecule incorporated or an endogenously biotinylated plant peptide.

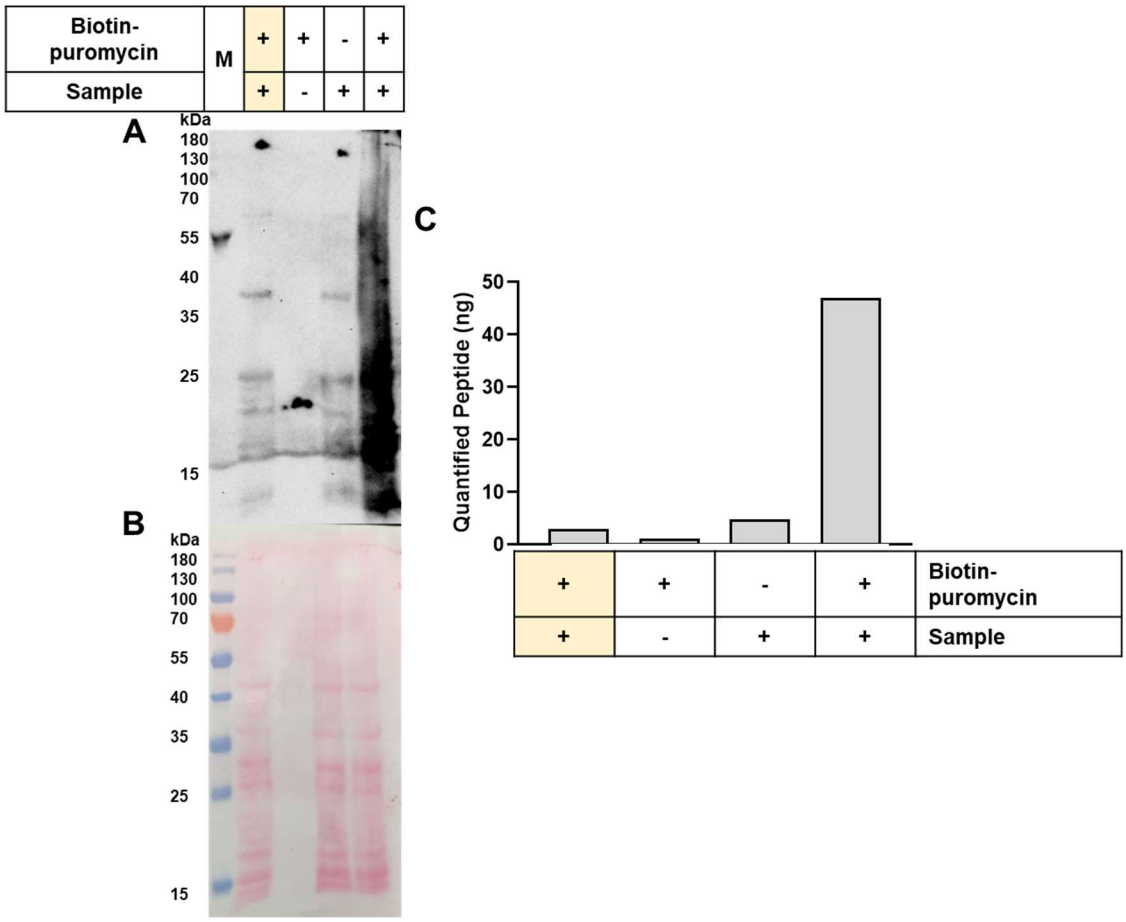

Figure 10: Unincorporated Biotin-Puromycin Does Not Generate Immunoblot Signal.

A) Immunoblot and B) Ponceau stain of immunoblots of samples with varying sample amount and biotin-puromycin incorporation. Lane table cells highlighted in yellow indicate sample where biotin-puromycin was added after SDS denaturation of sample ribosomes and peptides. Since biotin-puromycin in these lanes was added after sample denaturation, it would not incorporate into a peptide chain.

C) Peptide quantification of lanes in A based on a biotinylated-BSA curve.

M=molecular size marker.

3.6.2 Blot Exposure Time is Not a Key Factor in Quantification

In this experiment, I explored whether the exposure time of the blot confounds the quantification of puromycylated peptide (Fig. 11). Here, panels A through D present the same blot with images taken at increasing exposure times, 30 to 120s, accounting for the increase in signal (Fig. 11G). Note that these blot signals are not saturated in signal; any areas of saturation would be highlighted in red by the Imagelab program used for analysis. Evidently (Fig. 11F), large differences in exposure time (4-fold) only account for small differences in peptide quantification (~20%), as long as the samples are compared to a biotinylated BSA curve present on the same immunoblot.

Figure 11: Immunoblot Quantification is Not Affected by Slight Variances in Exposure Time.

A) 30s B)60s C)90s D) 120s exposures of a streptavidin-HRP probed immunoblot. Signal intensity increases with increased exposure. Biotinylated BSA and sample signal increase proportionally, allowing for accurate quantification. Note that immunoblots are not saturated with signal, saturated areas would be highlighted in red by Imagelab software.
E) Ponceau stain of blot in A-D. Protein loading is not equivalent between sample lanes, however, this experiment is used to show the effects of increased blot exposure, not differences in sample quantification.
F) A comparison of blot peptide quantifications of samples in A-D. Peptides were quantified using the signal form biotinylated-BSA present on the right side of the blots shown. Sample signal and biotinylated BSA curves form the same exposure times were used for quantification.
G) A comparison of western blot intensity values (AU) used for quantification for panels A-D. Y axis is on a log scale.
M= molecular weight marker.
B= blank lane containing only SDS loading buffer.

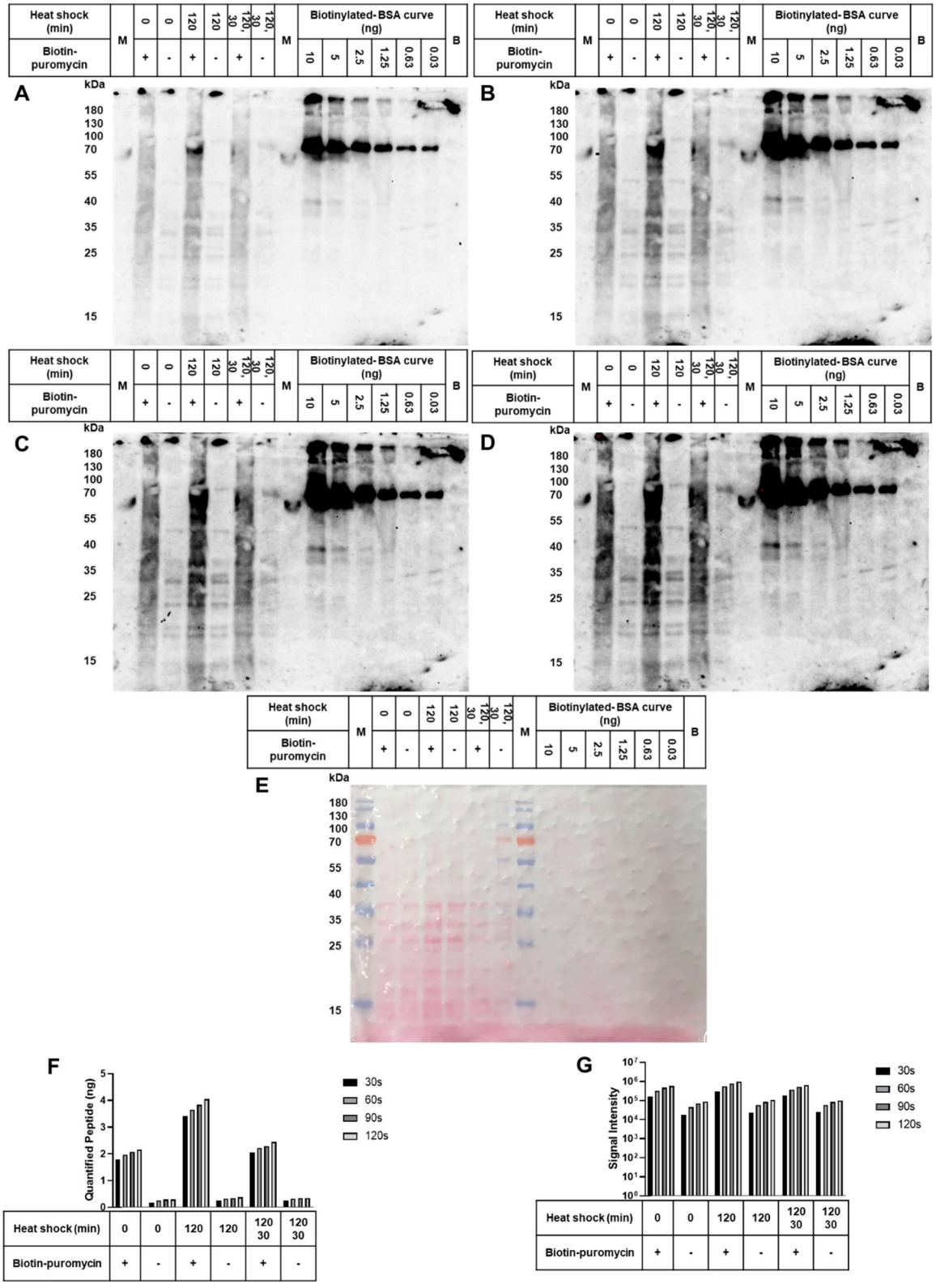
A
B
C
D
E
F
G
kDa
180
130
100
70
55
40
35
25
15
Heat shock (min)
Biotin-puromycin
M
Biotinylated-BSA curve (ng)
10
5
2.5
1.25
0.63
0.03
B
0
120
30
120, 30
+
-
Quantified Peptide (ng)
Signal Intensity
30s
60s
90s
120s

3.6.3 Freeze-Thaw Cycles Degrade Ribosome Puromycylation Activity

It is often convenient to store ribosomes at -80ºC after they have been isolated from the sucrose cushion. I tested whether freezing and thawing is detrimental for ribosomal activity in the subsequent puromycylation reaction. Figure 12 shows the decrease in puromycylation as a ribosomal sample undergoes one or two freeze/thaw treatments (Fig. 12A, B). Since large amounts of puromycylated peptides of all ranges are desirable for downstream experiments, a ribosomal sample that has never been frozen at -80°C is best used for maximum peptide production.

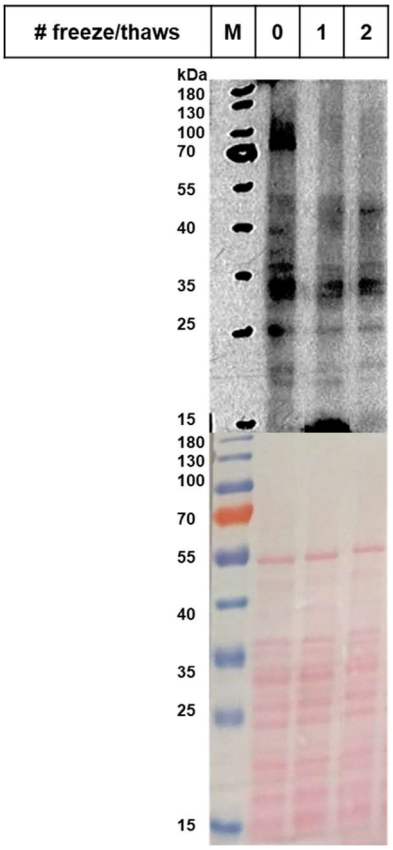

Figure 12: Ribosomes Lose Puromycylation Activity After Freeze/Thaw.

A) X-ray film of immunoblot and B) Ponceau S stain of samples that underwent subsequent freezing and thawing. Thawing was done at 4°C on ice and re-freezing was done by dipping sample tubes into liquid nitrogen. This experiment was not quantified because of issues with quantification on X- ray film.

M= Molecular size marker.

3.6.4 Western Blot Yields Reproducible Estimates of Puromycylation Activity

Heat stressed plant samples consistently contain fewer actively translating ribosomes (Fig. 13), consistent with the compromised translational state of the plant, while translation activity recovers are return to 22ºC for 30 min. The quantification of western blots has been found to be reproducible.Figure 13 shows multiple biological replicates quantified using this method. Reproducibility in quantification is maintained by only comparing sample signals to the BSA curve on the same membrane. Moreover, blank subtraction, meaning a lane of same size with no sample present, is required for accurate quantification. Variations in the yield of peptides may be attributed to sample freshness, as discussed in section 3.6.3, or uneven transfer of proteins across a blot.

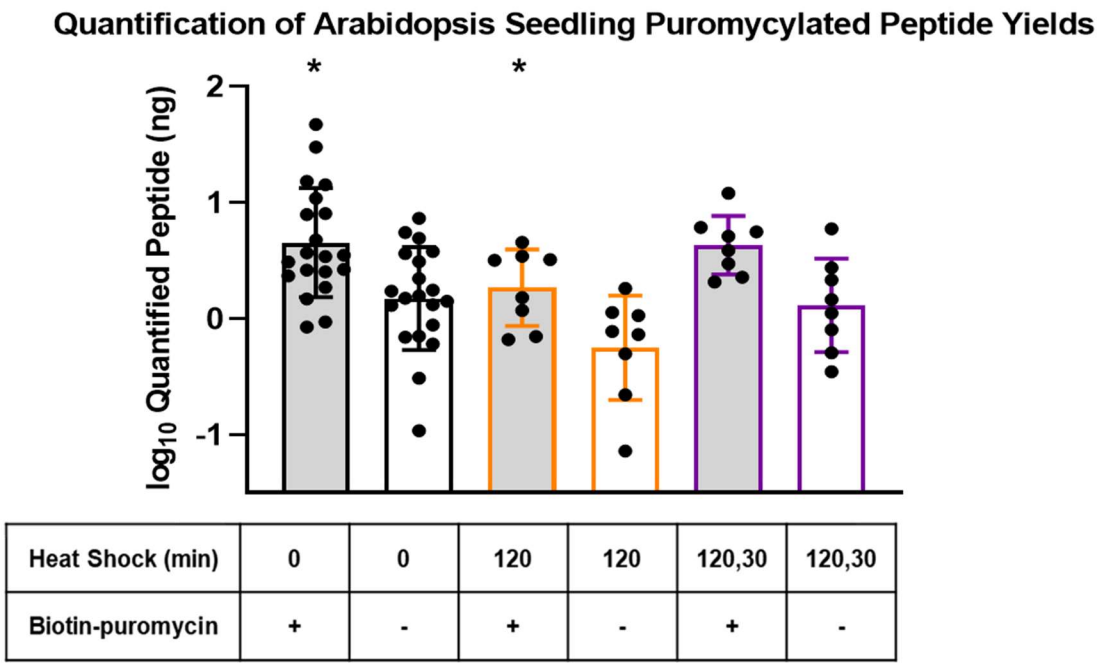

Figure 13: Quantification of Puromycylated Peptide Yields Between Untreated (0), Heat Stressed (120min) and Recovered (30min) Arabidopsis Samples.

120,30 samples indicate Arabidopsis that were treated with 120 min in heat, with a 30 min recovery period. Data points shown are biological replicates. * Welch's T test, $p < 0.05$. Note log-scale on y-axis.

3.6.5 Biotin-Puromycin Reactions Can be Scaled Up

Most reactions up until this point contained 20 micrograms of ribosomal RNA. In order to estimate how much puromycylated peptides are generated in larger scale reactions, as later used for LC-MS/MS analysis, reactions were scaled up two- to three-fold, while keeping the concentration of biotin-puromycin consistant at 100 pmol/μL. The quantification of these scaled reactions shows that the amount of biotin containing peptides increases proportionally to the amount of ribosomal sample used (Fig. 14A, B, C). Thus, the amount of puromycylated peptides in larger reactions may be predicted from smaller reactions.

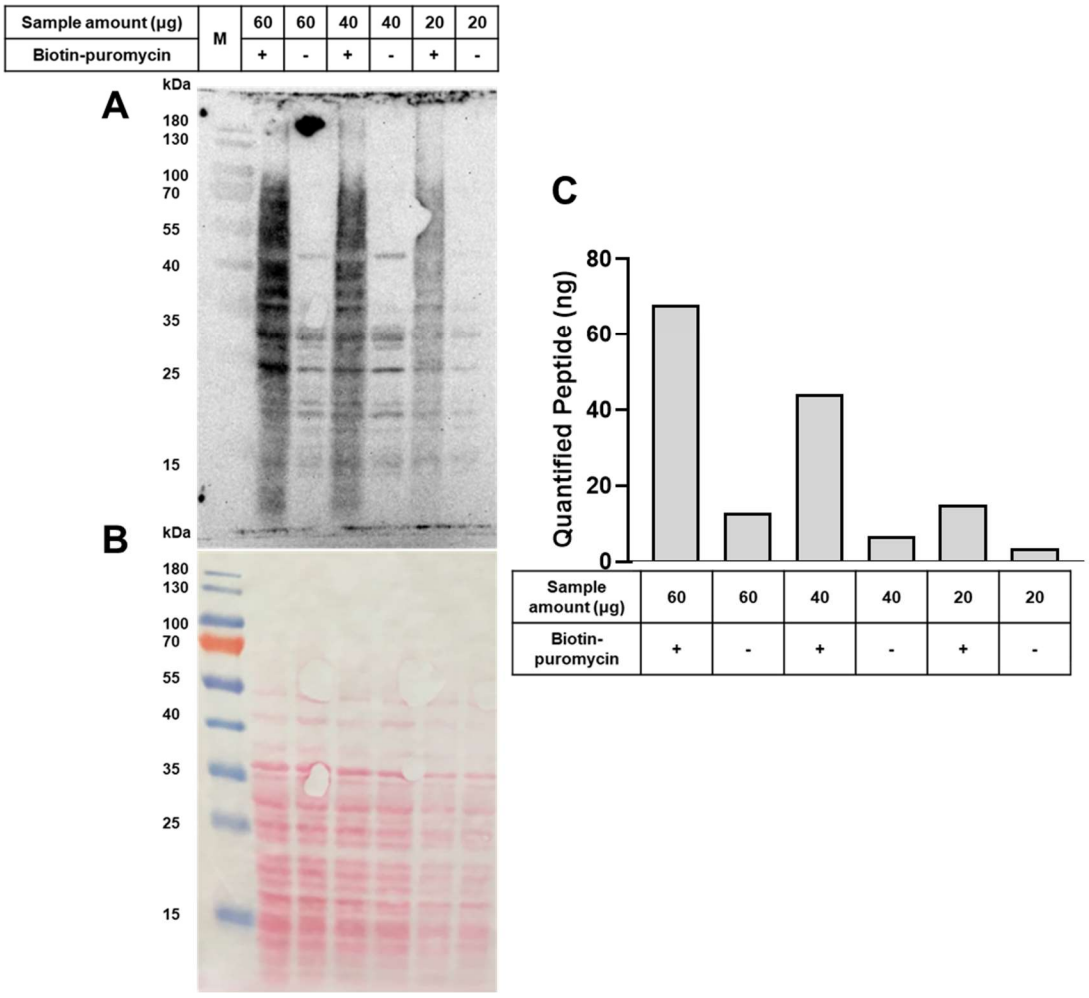

Figure 14: Puromycylation Reactions Scale Up in a Predictable Way.

A) Immunoblot and B) Ponceau stain of scaled-up puromycylation reactions containing increased amounts of ribosomal sample. Note that the order of samples loaded is from 60ng to 20 ng left to right. Biotin-puromycin concentrations in these reactions was maintained at 100µg/µL reaction.

C) Quantification of sample lanes in A.

M=molecular size marker.

3.6.6 Scaling of Puromycin Amount

In order to optimize the amount of biotin-puromycin in the puromycylation reaction, varying amounts of puromycin were used in reactions containing 20 micrograms of plant ribosomal sample. Although the yield of puromycylated proteins increased slightly with increasing puromycin, (Fig. 15 A, B, C) it must be considered that in downstream experiments excess biotin-puromycin needs to be removed prior to biotin-streptavidin affinity capture because unincorporated biotin-puromycin competes with biotinylated peptides for streptavidin binding sites. Therefore, a subsaturating concentration of biotin-puromycin, 1 µL/ 20 µg RNA, is used in all other puromycylation reactions for western blot and sample prepared for streptavidin bead capture.

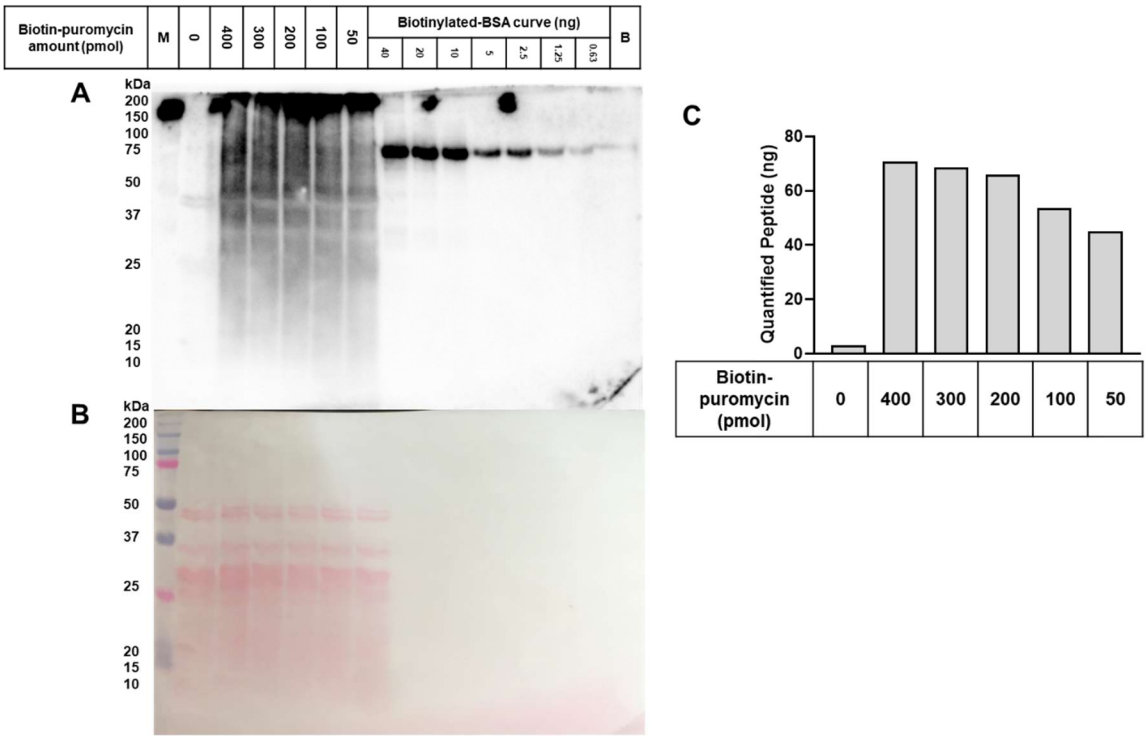

Figure 15: Reaction Yields Vary with Changes in Biotin-Puromycin Amount.

A) Immunoblot and B) Ponceau stain of sample reactions containing increased amounts of biotin-puromycin. C) Quantification of peptide signals from A).

M= molecular size marker.

3.6.7 Pea Seedling Ribosomes Have Strong Puromycylation Activity

It was found that pea 12-day old seedlings yield more ribosomes per unit fresh weight (Fig. 5). Their activity and puromycylation status were examined in Figure 16. Compared to 12-day old Arabidopsis seedlings, pea ribosomes have approximately 10-fold stronger puromycylation activity (Fig. 16A, B), whereas the amount of endogenous biotinylated proteins is only slightly increased.

In summary, these data demonstrate that ribosomes from both Arabidopsis seedlings and pea seedlings are active in tagging nascent peptides with biotin-puromycin. While puromycylated nascent peptides exceed the level of endogenous biotinylated proteins in both species, pea ribosomes are isolated at much higher yield and are also more active in puromycylation than those from Arabidopsis. The reasons for this difference are unclear at this time.

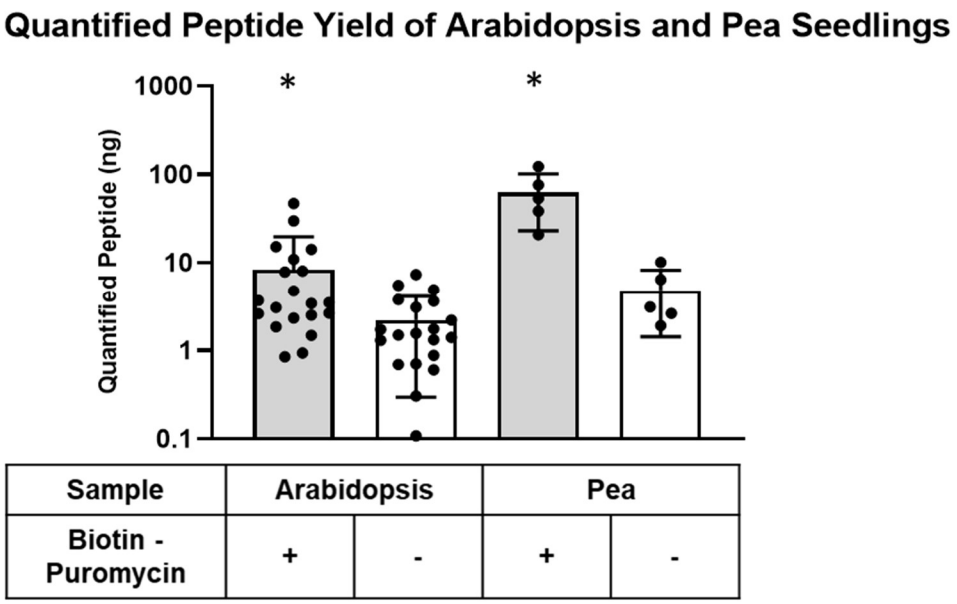

Figure 16: Pea Puromycylation Reactions Yield Larger Amounts of Puromycylated Peptides Than Those from Arabidopsis Seedling Ribosomes.

Reactions containing 20 micrograms of ribosomal RNA for each sample type were quantified for comparison. * Mann-Whitney Test, $p < 0.001$. Y-axis is in log-scale.

3.7 Bead Capture of Puromycylated Peptides and Proteomics

Having optimized the biotin-puromycin labeling of nascent peptides from Arabidopsis and pea seedlings, the next goals were to capture the peptides on streptavidin beads and to identify the captured peptides using LC-MS/MS analysis.

3.7.1 Streptavidin Bead Capture of Puromycylated Peptides is Optimized by Desalting and Denaturation

Streptavidin bead capture was optimized for Pierce Dynabeads, M280. We chose magnetic beads because these beads can be pelleted easily and efficiently during the numerous washing steps. In addition, other beads used in preliminary work suffered from non-specific binding of non-puromycylated proteins, which we aimed to resolve by using this new reagent.

Preliminary experiments had suggested that the capture of puromycylated proteins by the streptavidin beads was inhibited by unincorporated biotin-puromycin competing for binding sites on the streptavidin bead. Therefore, the puromycylation reaction was desalted to remove excess biotin-puromycin. In addition, 2M urea was added to the reaction as a denaturation step to aid in the release of puromycylated peptides form the ribosomes. These steps did not per se reduce the recovery of puromycylated peptides (Fig. 17A, lanes 7 and 6). While the capture lane still contains some peptide signal, these bands are very similar to the bands shown in non-puromycylated sample lanes (Fig 17 B, lane 8) indicating that puromycylated peptides are binding to the streptavidin beads with more efficiency than the endogenously biotinylated plant proteins once desalting and denaturing steps are included in sample preparation. This may be due to the positioning of the biotin moiety in the protein, making it inaccessible for streptavidin binding on beads. These peptides can however be detected on western blots since they are denatured on the SDS PAGE. Steps for bead

capture optimization are shown in Figure 17. Here, the effect of desalting columns and denaturation steps show an increase in binding efficiency of puromycylated peptides to streptavidin beads (Fig.17 lanes 6 and 7). These steps without bead capture slightly diminish signal of peptide available for capture, but the western blot signal is still much greater than the flow through loaded for bead capture steps. In summary, these experiments show the need for a desalting step as well as a denaturing step to increase puromycylated peptide capture.

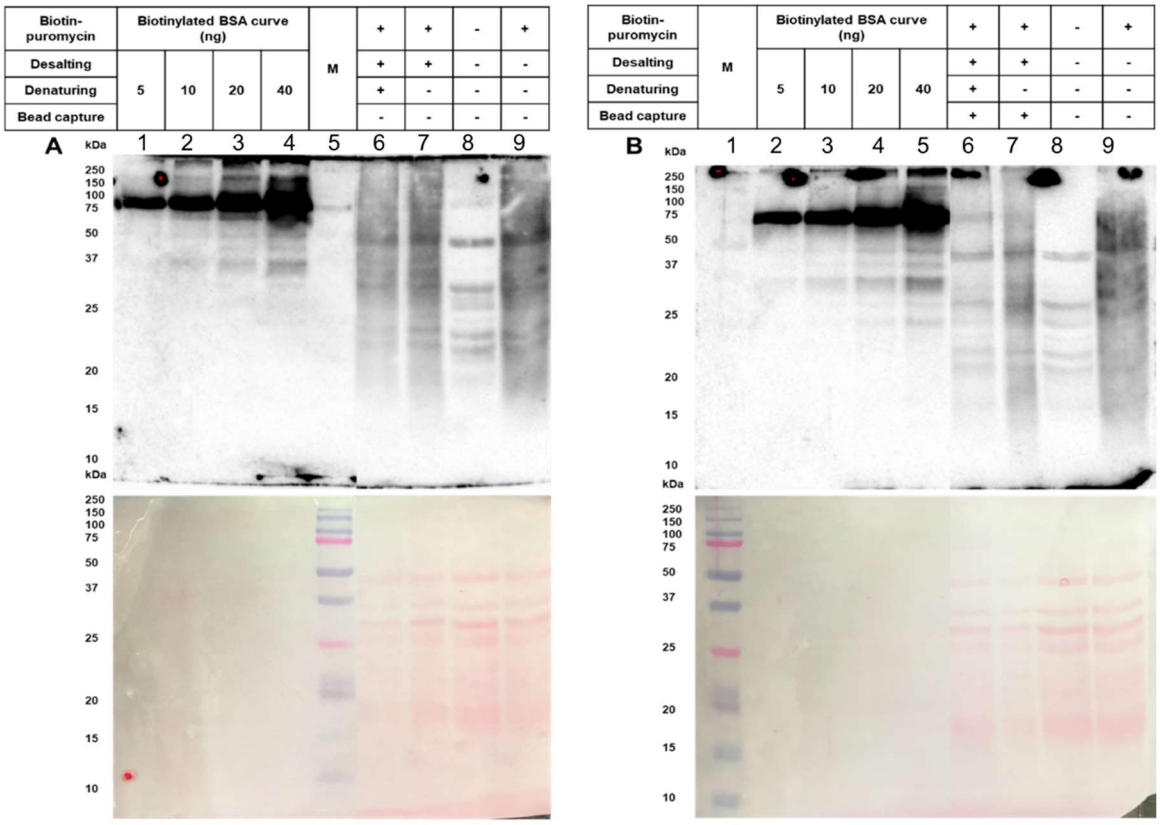

Figure 17: Streptavidin Bead Capture is Optimized with Sample Desalting and Denaturation Steps.

A) Lanes 7 and 8 show only slight loss of sample signal intensity after desalting and denaturation steps as compared to control puromycylation reaction lane 9

B) Lane 7 and 8 show bead capture flow through loaded, where a decrease in sample signal indicates increased binding to streptavidin beads.

M=molecular size marker.

The efficacy of using a desalting column was also shown in an experiment using biotinylated BSA (Fig. 18) Here, 50ng of BSA was used as a control in lane 1. Lane 3 shows streptavidin bead supernatant loaded. Here, absence of biotinylated BSA signal is due to protein capture on streptavidin beads. In lane 4, 50ng of biotinylated BSA, with biotin puromycin added underwent bead capture. This bead capture was unsuccessful, most likely due to the free-floating biotin puromycin competing for streptavidin binding sited with biotinylated BSA. In lane 2, excess biotin puromycin was removed with a desalting column and biotinylated BSA was once again able to bind to streptavidin beads, leaving no protein in the supernatant which was loaded on to the gel.

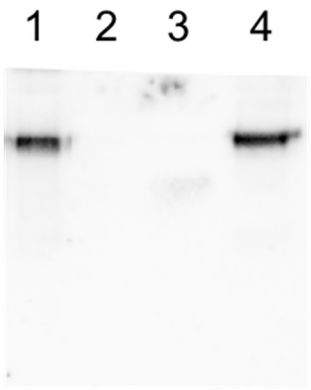

Biotinylated BSA (50 ng)	+	+	+	+
Biotin-puromycin	-	+	-	+
Desalting	-	+	-	-
Bead capture	-	+	+	+

Figure 18: Confirmation of Desalting Efficacy with Biotinylated-BSA.

50 ng of biotinylated BSA was used as a signal control. Biotin-puromycin was spiked into the protein to show that excess of this reagent prevents successful binding of biotinylated protein to streptavidin beads. Biotin puromycin that was spiked in can be removed from the protein via a desalting column step.

3.7.2 Pea Seedling Samples Used for LC-MS/MS Contained Succesful Puromycylation Reactions and Bead Captures

In preparation for LC-MS/MS analysis, pea ribosomes were subjected to puromycylation in two technical replicates alongside non-puromycylated negative controls. Reaction products were desalted and were verified for their puromycylation reaction efficiency and peptide capture on streptavidin beads (Fig. 18). Samples were from 12-day-old pea seedlings grown at room temperature and harvested on the same day. As shown in Fig. 18A and B, there was no loss of puromycylated sample in the desalting column. The bead-capture flow-through lanes show a decrease of signal in the puromycylated samples, indicating that peptides have bound to beads. Proteins that have remained in solution (lanes 4 in Fig. 18A and C) appeared to be enriched for native biotinylated proteins and contained the bulk of ribosomal protein, as expected (Ponceau S stain). The puromycylated peptides appear to be firmly bound to the beads because the first wash with SDS-urea buffer released only negligible amounts (lanes 5). In the non-puromycylated control reactions it appears that the native biotinylated proteins again did not bind efficiently to the beads under the given conditions (Fig. 18B). This may be happening because the biotin moiety is buried inside the tertiary structure. For practical purposes, if native biotinylated proteins are selected against, this would favor the detection of nascent chains, which have their biotin exposed at the C-terminus.

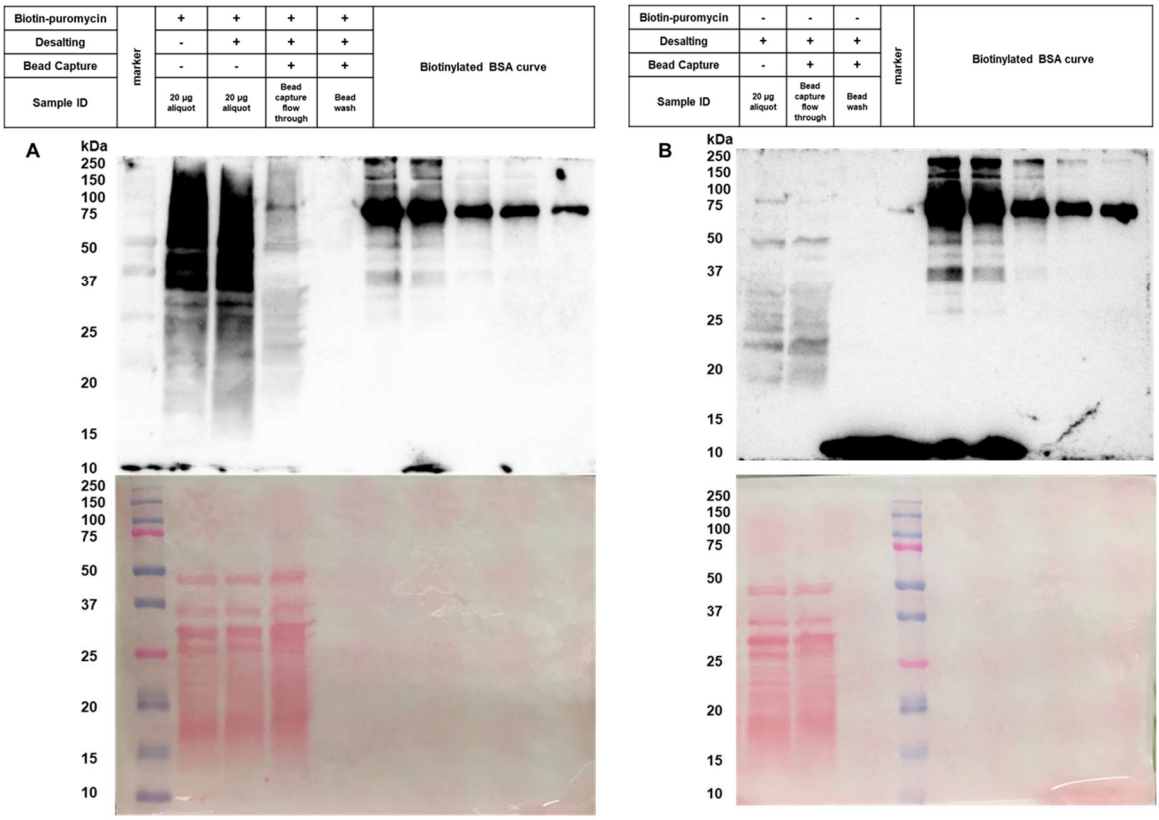

Figure 19: Bead Capture of Puromycylated Peptides Can be Confirmed Using Western Blotting.

Ribosomes equivalent to 520 micrograms of ribosomal RNA were puromycylated and aliquots equivalent to 20 micrograms were analyzed by immunoblotting. A and B show immunoblots of samples prepared on 110719 sent for LC-MS/MS analysis. A shows puromycylated samples while B shows non-puromycylated controls. Lanes show the efficiency of puromycylation reactions, their desalting, as well as efficiency of bead binding and wash steps.

3.7.3 Puromycylated Peptide Samples Analyzed via LC-MS/MS Contain a Wider Variety and a Greater Abundance of P than Non-puromycylated Samples

The two technical replicates of puromycylation reactions alongside with their non-puromycylated controls (Fig. 18), as well as another two puromycylation reactions processed two months earlier as a biological replicate, were captured on streptavidin beads, washed, subject to on-bead trypsin digestion, and peptides were analyzed by LC-MS/MS as described under Methods. The wet-lab analysis and initial mapping of the peptides to *Pisum sativum* gene models were performed by Dr. Paul Abraham at Oak Ridge National Lab. Subsequent bioinformatic analyses in this chapter are based on the supplemental data tables in the attachments.

A summary of the number and abundance of peptides detected in each sample is shown in Table 2. This table shows that the puromycylated samples yielded approximately 1000 additional peptides over the non-puromycylated samples. The total peptide signal was also more abundant in the puromycylated samples as was the abundance of the median peptide. These results show that there is significant non-specific binding of non-puromycylated peptides to the beads. However, a substantial fraction of the >2,000 peptides detected appears to be puromycylated, suggesting that they are nascent peptides. Here, streptavidin, which is the binding moiety to which biotin-puromycylated peptides bind to is used as a proxy for overall sample digestion. According to the recovery of streptavidin peptides, the efficiency of digestion and mass spectrometric detection was similar between puromycylated and non-puromycylated samples (Table 2).

The samples provided and their replicates are listed. 1 (+P), 2 (+P) 3(+P) and 4(+P) are technical replicates of bead capture done on different dates. All samples are puromycylated, denoted by the (+P). (-P) denotes samples that did not undergo puromycylation reactions. These samples would establish a kind of background signal to compare other experiments to as the only peptides that would be captured should be those that are endogenously biotinylated or that have some other kind of affinity to the magnetic beads.

Table 2: Summary of Samples Analyzed via LC-MS/MS.

Sample signal intensity refers to the abundance of overall peptide signal detected. Sample IDs will be referred to in all following figures for clarity.

Sample ID	# unique peptides detected	Signal intensity, sum of all peptides (E+10)	Signal intensity, median peptide (E+5)	Signal intensity, sum of all streptavidin peptides(E+10)
1 (+P)	2115	2.27	3.95	0.35 (15.4%)
2 (+P)	2122	1.68	4.98	0.35 (20.9%)
3 (+P)	2258	2.67	9.91	0.23 (8.5%)
4 (+P)	2169	1.11	3.87	0.13 (11.5%)
1 (-P)	1452	0.96	1.72	0.19 (19.6%)
2 (-P)	1424	1.251	2.69	0.20 (15.8%)

In Figure 20, technical replicates of the sample experiments are compared to each other (Fig. 20A-D). Panels A and B compare the two sets of puromycylation reactions done on different dates. Panel C compares the averages of these two technical replicates as grouped by date of peptide capture. Comparison of the average peptide abundances between the two biological replications of puromycylated samples also shows fairly consistent results (Fig. 20 C, R^2=0.75). Given the delay in processing samples +1 and +2, this result also shows that the peptides are stably bound to the streptavidin beads and that, when samples are stored at 4°C they do not degrade. However, the exact time frames needed between puromycylation reaction, bead capture and analysis were not investigated.

In panel E, average puromycylated and non-puromycylated peptide abundances are compared. Puromycylated samples yield a broader range of peptides, and these peptides are generally more abundant than in non-puromycylated reactions. This indicated that puromycylation reactions were successful, although there is also a significant background of non-specific capture of mature pea proteins as indicated from the non-puromycylated samples.

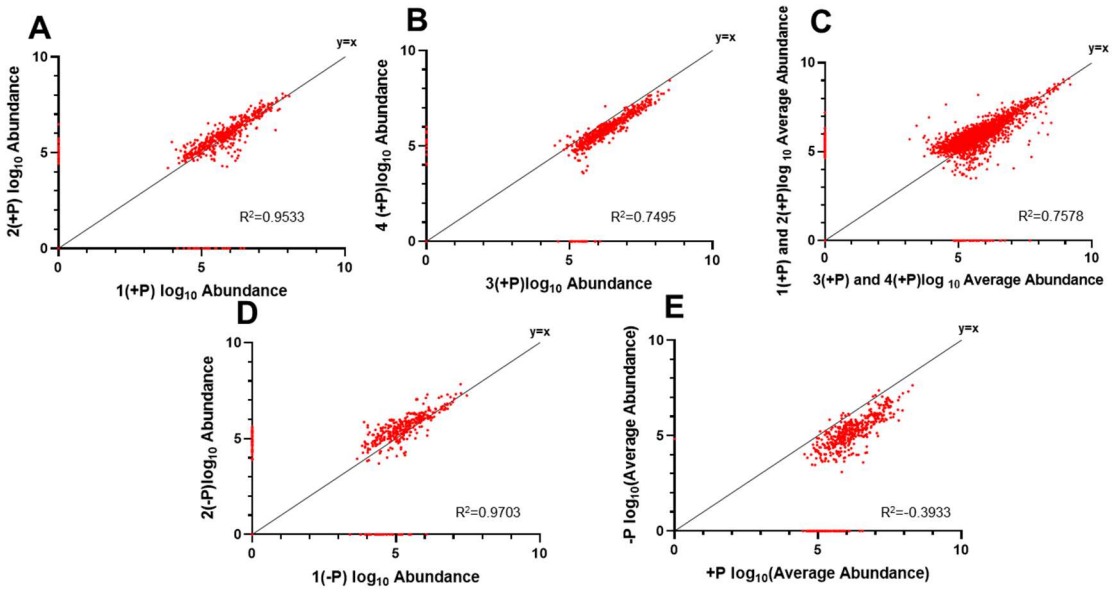

Figure 20: Puromycylated Peptides are More Abundant and Varied than Non-Puromycylated Peptides.

A) Comparison of technical replicates of puromycylated bead captures done on 101719. These peptides bound to streptavidin beads were stored at 4°C until analyzed with other samples on 111719.

B) Comparison of peptide abundance of puromycylated peptide capture technical replicates done on 110719

C) Comparison of non puromycylated sample bead capture technical replicates

D) Comparison of puromycylation technical replicates performed on different dates but analyzed at the same time, shown in A) and B)

E) Comparison of puromycylated and non puromycylated average peptide yields

Note that axes are in log scale. All peptides that were not detected in one sample were assigned an abundance of 1 so they could be plotted on the log scale.

+P, puromycylated samples, -P non puromycylated samples.

Refer to Table 2 for sample abbreviations.

Peptides at abundance of 1 were excluded from R^2 calculations

The peptides detected were then mapped to *Pisum sativum* gene models as previously described (Chapter 2.1) in order to estimate which proteins are being detected. During BLAST searching, it was found that peptides may map to multiple paralogs of proteins in the pea genome. These paralogs were examined for their identity and the one with the most peptides mapped to it with 90% identity was chosen to be the representative protein for its paralogs. Table 3 describes the signal abundance due to proteins detected in each sample.

Table 3: Sample Signal Based on Peptides Mapped to Pea Proteins

Sample ID	# unique proteins detected	Signal intensity, sum of all proteins (E+8)	Signal intensity, median protein (E+4)
1(+P)	514	18.5	45.6
2(+P)	522	23.7	53.1
3(+P)	559	52.7	13.9
4(+P)	550	21.1	5.88
1(-P)	373	3.05	3.29
2(-P)	387	5.60	9.59

The approximately 500 proteins detected in the puromycylated samples were then functionally classified for their presumptive cellular location by gene ontology analysis [34]. In the puromycylated samples, about 29% of the proteins were of chloroplast origin and 19% were ribosomal (Fig. 21). In the non-puromycylated control these fractions were approximately similar. This is not unexpected, because the non-puromycylated background proteins will represent highly abundant cellular proteins, and these proteins are also expected to be most actively translated and thus represented in the form of puromycylated nascent peptides.

Peptide abundances separated by GO term are further shown in Figure 22. As in Figure 21, chloroplast, ribosome and unspecified (other) proteins show the most capture by streptavidin beads. All panels A-E show an enrichment of protein detection in puromycylated samples as compared to non puromycylated controls.

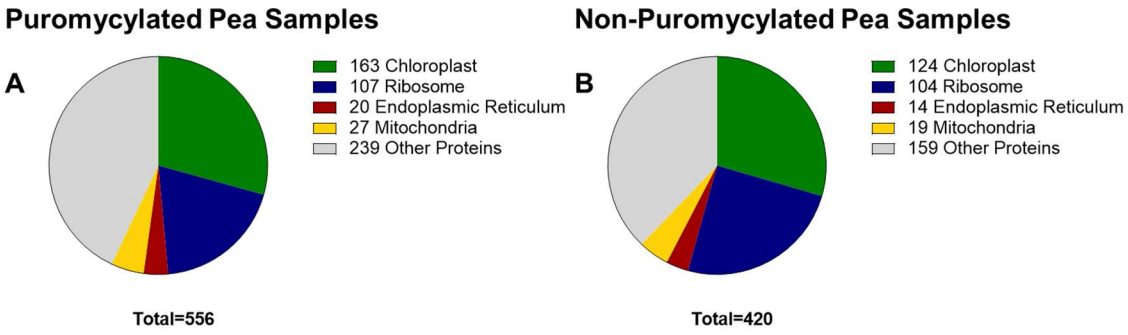

Figure 21: Puromycylated Peptide Capture Yields a Greater Amount of Detectable Proteins than Non-Puromycylated Samples

GO cell compartment analysis of A) puromycylated and B) non puromycylated pea bead captures resulting from LC-MS/MS.

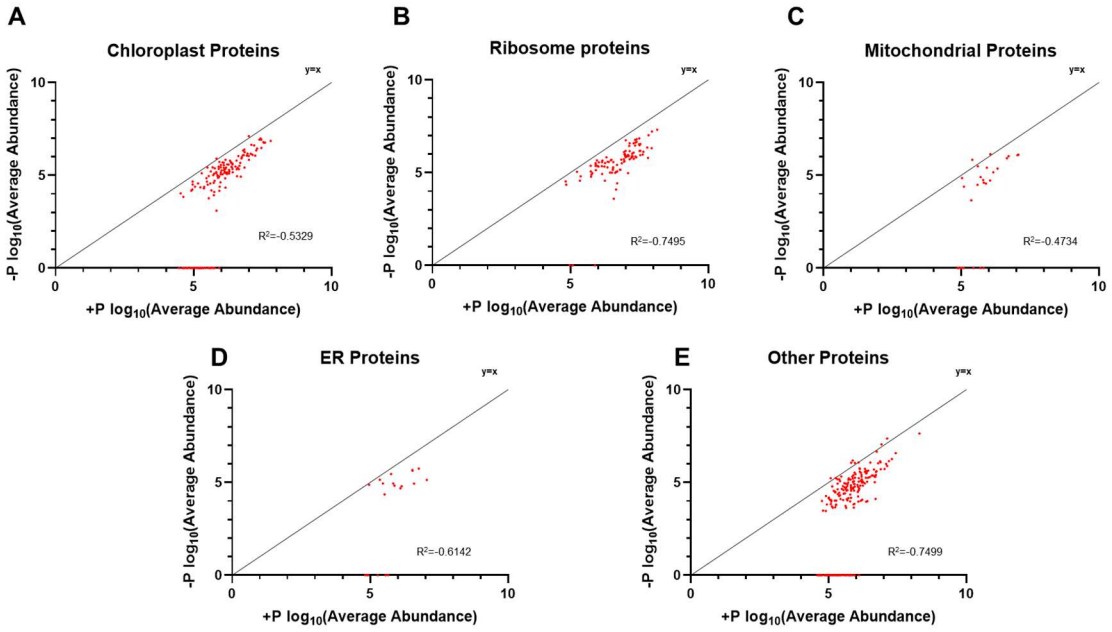

Figure 22: Abundance of Proteins in Puromycylated and Non-Puromycylated Samples Based on GO Cellular Location.

Puromycylated and Non puromycylated average abundance comparisons of proteins found in different cellular locations.

Axes are in log scale.

The proteins of special interest for analysis were ones which were newly translated. The detection of these proteins could serve as an indicator for the rate of translation of these specific peptides. Therefore, proteins with a transit peptide were a priority in PUNCH-P analysis, since transit peptides would only be present in peptides which had been in the process of translation and had not yet traveled to their destination organelle.

Most chloroplast proteins are known to be targeted to the chloroplast via an amino-terminal transit peptide [32]. Transit peptide information for these proteins was not available for *Pisum sativum,* however transit peptide regions of FASTA sequences of proteins of interest were predicted using ChloroP servers. The predicted transit peptide lengths are shown as a yellow highlighted region in Figure 21. Peptide positions and abundances were mapped to FASTA sequences of proteins containing transit peptides (Fig 21). Red points show the start of alignment of puromycylated peptides, while black points show non puromycylated peptides. In all figures, puromycylated peptides are overall more abundant than non puromycylated peptides. However, many peptides in puromycylated and non puromycylated samples have the same position, indication that these proteins are detectable in similar lengths and stage of translation in both sample types. However, in panels B, D, and I, puromycylated peptides are enriched in the transit peptide region of the protein. A caveat in this data interpretation is the assumption that none of these peptides have had any N terminal cleavage during translation. It also assumes that there is no bias in capture efficiency of the biotin-puromycylated proteins and that they underwent equivalent tryptic digest prior to LC-MS/MS analysis.

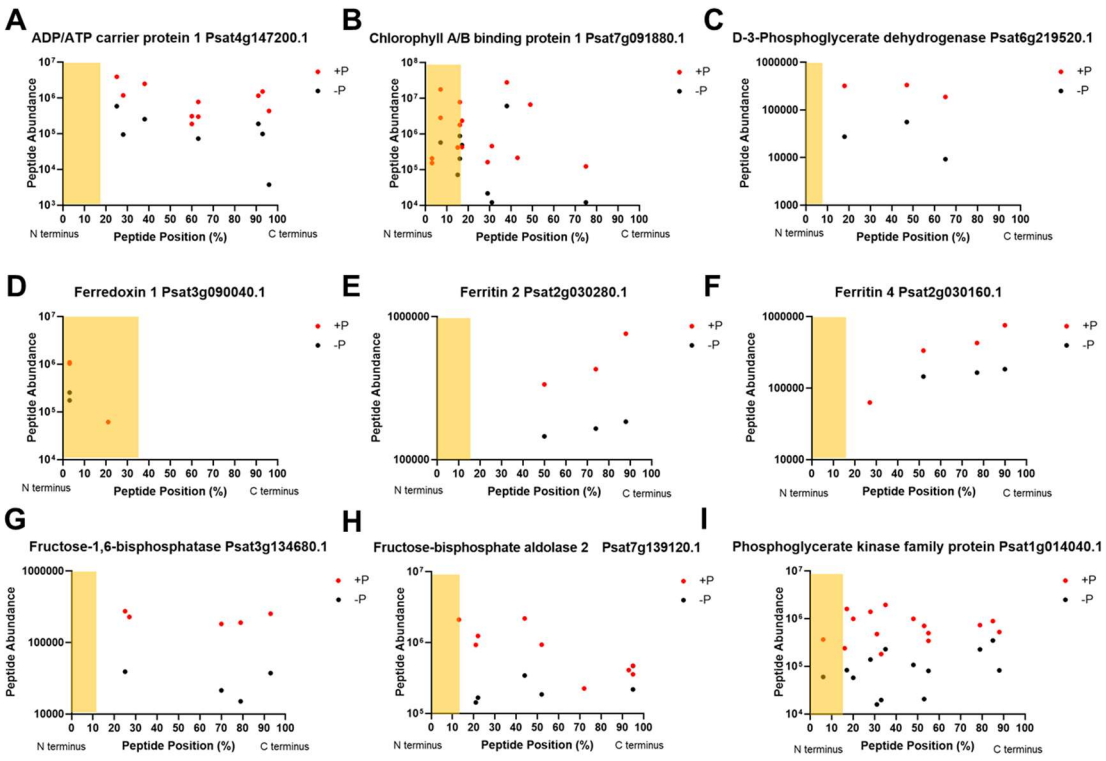

Figure 23: Peptide mapping of transit peptide containing proteins detected using PUNCH-P.

Peptides were mapped based on their % position along the protein length. X axes are represented as % of full peptide length with 0 being the N terminus and 100 being the C terminus. This standardizes the mapping of peptides regardless of protein amino acid length. Red points denote puromycylated peptides, black points denote non puromycylated peptides. Y axis is in a log scale.

4. DISCUSSION AND CONCLUSIONS

In this work, I show for the first time that the PUNCH-P technique may be applied to plant samples. After optimizing various steps of the puromycylation protocol using Arabidopsis seedlings and flowers, it was shown that pea seedlings not only produce up to 10-fold more ribosomes than Arabidopsis (Fig. 5), but also yield higher amounts of puromycylated nascent peptides per ribosome as compared to Arabidopsis. This may be due to the large amounts of translational activity necessary for the development of the 12-day old pea seedlings.

These plants types have also shown to be translationally affected by heat stress. Pea and Arabidopsis seedlings both exhibit polysomal collapse after 2-hour heat shock at 37°C, and regain their polysomal activity after a 30-minute recovery period (Fig. 6). These results support results found in literature and provide an easy plant treatment that affects translational activity to perform for future PUNCH-P experiments.

This work also shows the efficacy of puromycylation reaction on ribosomes extracted from varying plant tissues (Fig. 16). Both pea and Arabidopsis seedlings were able to be puromycylated using the puromycylation techniques optimized in Figures 10-15. These experiments showed the robustness of the puromycylation reaction and determined factors, such as presence of KCl and sample freshness that determine the yield of puromycylated peptides form a puromycylation reaction.

In order to quantitatively compare puromycylation reactions, I adopted biotinylated BSA as a standard curve on my western blots. I also used a luminescence imager and Imagelab software, a step up from X-ray film qualitative imaging methods, in order to better quantify the recovery of puromycylated nascent peptides. These quantification methods have been shown to be replicable and can be applied to a variety of samples (Fig. 11,13,16).

I applied my western blot quantification method on heat stress samples to investigate what proteins were affected by heat shock. I found that heat stress reduces the bulk of puromycylated proteins, as expected based on the polysome collapse seen using traditional polysome fractionation. Puromycylation after heat shock also produced bands that may reflect the positions of known heat shock proteins. Bands that are unaffected remain those that are found in non-puromycylated sample (Fig. 9).

After confirming my puromycylation reaction, the effect of heat shock on plant samples, and my methods of quantifying the amount of nascent peptides labeled by a puromycylation reaction, I developed an optimized streptavidin bead capture method for the puromycylated peptides (Fig. 17). The bead capture step of desalting was found to be necessary because unincorporated biotin-puromycin, competes with the puromycylated nascent peptides for efficient binding to beads. Denaturation steps using SDS and urea buffer was also needed to more efficiently capture puromycylated peptides. However, it is still seen based on these blots that endogenously biotinylated peptides, reflected in non-puromycylated control lanes are still not being captured by the streptavidin beads. I hypothesize that this is due to the location of their biotin moiety, which may be tucked into the protein structure in such a way that it is inaccessible for streptavidin binding. Harsher denaturing steps may be needed for their nascent proteins for their efficient capture.

Although it was found that non-puromycylated peptides continued to bind to the beads non-specifically, the recovery of puromycylated nascent peptides was several-fold higher in puromycylated versus non-puromycylated peptides abundances, and many peptides were unique to the puromycylated samples (Fig. 19). After mapping detected peptides to protein sequences, it was found that over 500 proteins or protein families were detected as nascent proteins. The number of background proteins, found in non

puromycylated capture samples, binding non-specifically to the beads was smaller, and these proteins were also less abundant on average. Proteins detected also vary between puromycylated and non-puromycylated peptides.

Proteins detected based on their captured peptide fragments were also mapped to their organelle of origin based on GO analysis (Fig. 20, 21). While ratios of organellar peptides captured remained similar between puromycylated and non puromycylated samples, the puromycylated samples yielded much more abundant sample signals. These results show that puromycylation does indeed affect the efficacy of capture of peptides, however, there may yet be a bias towards a specific set of peptides since many of the same peptides were reflected in puromycylated and non puromycylated samples.

Peptide fragments resulting from LC-MS/MS analysis were also mapped to FASTA sequences of proteins which are known to have transit peptide sequences (Fig 22). The idea was, that peptides puromycylated mid-translation would still contain their transit peptide sequence and have more peptide abundance towards the N terminal region of the protein sequence. In this study, I saw only a few proteins with such a bias. This may be due to the few amounts of proteins mapped manually to their sequences, or the type of protein captured for analysis.

4.1 Future Work

Optimization of the PUNCH-P method should primarily focus on the expansion of the range of peptides and thus proteins detectable. As compared to Aviner et al, who detected thousands of proteins, in our hands the recovery of nascent peptides was less robust, detecting only about 500 proteins. To achieve a better recovery of quantifiable nascent plant proteins it would be easiest to start with more starting material, also using a larger amount of beads for peptide capture. Another approach would be to use streptavidin coated beads with more binding sites available. One major concern has been the rather extensive nonspecific binding of non-puromycylated proteins to the streptavidin beads, which has been observed with two different bead products. This extends beyond the abundant ribosomal proteins to proteins such as Rubisco, which is not even very abundant in the ribosome pellet. More stringent bead washing conditions should be explored, or possibly blocking non-specific binding sites with a generic non-plant protein.

Another factor for consideration is whether puromycin is incorporated randomly across the protein sequence or in some biased fashion. If it is incorporated randomly one would expect a strong bias against C-terminal peptides in the mass spectrometry. This is observed for some proteins but not all, using chloroplast proteins as a case in point. This may indicate that certain mRNAs have an excess of ribosomes on the 3' end of the ORF beyond what is expected if elongation speed were even across the mRNA., even in non puromycylated samples. This may occur as a result of bead capture bias, where some nascent proteins may bind more efficiently to streptavidin beads than others.

As PUNCH-P is optimized to yield, ideally, an alternative method to measure translational efficiency, this method should be used on other plant samples, such as

plants undergoing heat stress or hypoxia. PUNCH-P may shine with treatments that cause rapid drops in translation, because these would not lend themselves to alternative methods that require long labeling times such as SILAC. The use of mass spectrometry analysis of these heat-treated plants could also identify and quantify the rate of synthesis of different proteins that are known to be expressed during heat shock.

LIST OF REFERENCES

1. Aviner, R., T. Geiger, and O. Elroy-Stein, *Genome-wide identification and quantification of protein synthesis in cultured cells and whole tissues by puromycin-associated nascent chain proteomics (PUNCH-P).* Nat Protoc, 2014. **9**(4): p. 751-60.
2. Pestka, S., *Inhibitors of Ribosome Functions.* Annu. Rev. Microbiol., 1971. **25**: p. 487-562.
3. Aviner, R., T. Geiger, and O. Elroy-Stein, *Novel proteomic approach (PUNCH-P) reveals cell cycle-specific fluctuations in mRNA translation.* Genes & development, 2013. **27**(16): p. 1834-1844.
4. Calkhoven, C.F., C. Müller, and A. Leutz, *Translational control of gene expression and disease.* Trends in Molecular Medicine, 2002. **8**(12): p. 577-583.
5. Bailey-Serres, J., *Selective translation of cytoplasmic mRNAs in plants.* Trends in Plant Science, 1999. **4**(4): p. 142-148.
6. McLoughlin, F., et al., *Class I and II Small Heat Shock Proteins Together with HSP101 Protect Protein Translation Factors during Heat Stress.* Plant Physiol, 2016. **172**(2): p. 1221-1236.
7. Salome, P.A., *Some Like It HOT: Protein Translation and Heat Stress in Plants.* Plant Cell, 2017. **29**(9): p. 2075.
8. Echevarria-Zomeno, S., et al., *Regulation of Translation Initiation under Biotic and Abiotic Stresses.* Int J Mol Sci, 2013. **14**(3): p. 4670-83.
9. Basbouss-Serhal, I., et al., *Germination Potential of Dormant and Nondormant Arabidopsis Seeds Is Driven by Distinct Recruitment of Messenger RNAs to Polysomes.* Plant Physiol, 2015. **168**(3): p. 1049-65.
10. Hwang, J., et al., *Plant Translation Elongation Factor 1Bbeta Facilitates Potato Virus X (PVX) Infection and Interacts with PVX Triple Gene Block Protein 1.* PLoS One, 2015. **10**(5): p. e0128014.
11. Merchante, C., A.N. Stepanova, and J.M. Alonso, *Translation regulation in plants: an interesting past, an exciting present and a promising future.* The Plant Journal, 2017. **90**(4): p. 628-653.
12. Mignone, F., et al., *Untranslated regions of mRNAs.* Genome biology, 2002. **3**(3): p. REVIEWS0004-REVIEWS0004.
13. Zhang, L., et al., *Mutations in eIF5B Confer Thermosensitive and Pleiotropic Phenotypes via Translation Defects in <em>Arabidopsis thaliana</em&gt.* The Plant Cell, 2017. **29**(8): p. 1952.
14. Ha, S.-W., et al., *Rapidly Translated Polypeptides Are Preferred Substrates for Cotranslational Protein Degradation.* The Journal of biological chemistry, 2016. **291**(18): p. 9827-9834.
15. Kotak, S., et al., *Complexity of the heat stress response in plants.* Curr Opin Plant Biol, 2007. **10**(3): p. 310-6.
16. Chantarachot, T. and J. Bailey-Serres, *Polysomes, Stress Granules, and Processing Bodies: A Dynamic Triumvirate Controlling Cytoplasmic mRNA Fate and Function.* Plant Physiol, 2018. **176**(1): p. 254-269.

17. Yángüez, E., et al., *Analysis of Genome-Wide Changes in the Translatome of Arabidopsis Seedlings Subjected to Heat Stress.* PLOS ONE, 2013. **8**(8): p. e71425.
18. Vierling, E., *The Roles of Heat Shock Proteins in Plants.* Annual Review of Plant Physiology, 2003. **42**: p. 579-620.
19. Walters, R.W. and R. Parker, *Coupling of Ribostasis and Proteostasis: Hsp70 Proteins in mRNA Metabolism.* Trends Biochem Sci, 2015. **40**(10): p. 552-559.
20. Protter, D.S.W. and R. Parker, *Principles and Properties of Stress Granules.* Trends Cell Biol, 2016. **26**(9): p. 668-679.
21. Su, Z., et al., *Genome-wide RNA structurome reprogramming by acute heat shock globally regulates mRNA abundance.* Proceedings of the National Academy of Sciences, 2018. **115**(48): p. 12170.
22. Vogel, C. and E.M. Marcotte, *Insights into the regulation of protein abundance from proteomic and transcriptomic analyses.* Nat Rev Genet, 2012. **13**(4): p. 227-32.
23. Chassé, H., et al., *Analysis of translation using polysome profiling.* Nucleic acids research, 2017. **45**(3): p. e15-e15.
24. Roy, B. and A.G. von Arnim, *Translational Regulation of Cytoplasmic mRNAs.* Arabidopsis Book, 2013. **11**: p. e0165.
25. Aviner, R., T. Geiger, and O. Elroy-Stein, *Novel proteomic approach (PUNCH-P) reveals cell cycle-specific fluctuations in mRNA translation.* Genes Dev, 2013. **27**(16): p. 1834-44.
26. Glenn, W.S., et al., *Bioorthogonal Noncanonical Amino Acid Tagging (BONCAT) Enables Time-Resolved Analysis of Protein Synthesis in Native Plant Tissue.* Plant physiology, 2017. **173**(3): p. 1543-1553.
27. Ingolia, N.T., *Ribosome Footprint Profiling of Translation throughout the Genome.* Cell, 2016. **165**(1): p. 22-33.
28. Dermit, M., M. Dodel, and F.K. Mardakheh, *Methods for monitoring and measurement of protein translation in time and space.* Molecular bioSystems, 2017. **13**(12): p. 2477-2488.
29. Van Hoewyk, D., *Use of the non-radioactive SUnSET method to detect decreased protein synthesis in proteasome inhibited Arabidopsis roots.* Plant Methods, 2016. **12**: p. 20.
30. Dash, S., et al., *Legume information system (LegumeInfo.org): a key component of a set of federated data resources for the legume family.* Nucleic Acids Research, 2015. **44**(D1): p. D1181-D1188.
31. Madden, T., *The BLAST Sequence Analysis Tool*, in *The NCBI Handbook*. 2013, National Center for Biotechnology Information (US).
32. Chotewutmontri, P. and B.D. Bruce, *Non-native, N-terminal Hsp70 molecular motor recognition elements in transit peptides support plastid protein translocation.* J Biol Chem, 2015. **290**(12): p. 7602-21.
33. Emanuelsson O, N.H., von Heijne G, *ChloroP, a neural network-based method for predicting chloroplast transit peptides and their cleavage sites.* Protein Science, 1999. **8**(5): p. 978-984.

34. The UniProt, C., *UniProt: a worldwide hub of protein knowledge.* Nucleic Acids Research, 2018. **47**(D1): p. D506-D515.
35. Merret, R., et al., *Heat Shock Protein HSP101 Affects the Release of Ribosomal Protein mRNAs for Recovery after Heat Shock.* Plant Physiol, 2017. **174**(2): p. 1216-1225.
36. Nikolau, B.J., J.B. Ohlrogge, and E.S. Wurtele, *Plant biotin-containing carboxylases.* Archives of Biochemistry and Biophysics, 2003. **414**(2): p. 211-222.
37. M. Barbacid, M.F., D. Vazquez, *Inhibitors of Polypeptide Elongation on Yeast Polysomes.* The Journal of Antibiotics, 1972. **28**(6).

VITA

Aleksandra (Ola) Noras was born on October 4, 1995 In Wrocław, Poland. Her family moved to the US when she was 3 years old. She received her BS in Chemistry/ Biochemistry for the University of North Carolina at Greensboro in 2017 and started her MS in Biochemistry/Molecular Biology at the University of Tennessee -Knoxville in August of 2017. After finishing her master's degree, she plans on beginning her Fulbright fellowship to Poznan, Poland where she will begin research on barley heat and drought stress at Adam Mickiewicz University.